ADDENDUM TO THE ANNUAL TECHNICAL REPORT 1985

on

Earthquake Monitoring of Eastern and Southern Washington

September 1985

Crustal Structure of the Columbia Basin, Washington from Borehole and Refraction Data

by:

David W. Glover

A Master of Science Thesis

Geophysics Program

University of Washington

Seattle, Washington

8703160255 871212
PDR WASTE
WM-10 PDR

University of Washington

Abstract

CRUSTAL STRUCTURE OF THE COLUMBIA BASIN, WASHINGTON FROM BOREHOLE AND REFRACTION DATA

by David W. Glover

Chairperson of the Supervisory Committee: Professor Stephen D. Malone
Geophysics Program

A three-dimensional five-layered crustal model of the Columbia Basin has been constructed based on refraction data collected in August, 1984 by the USGS, Rockwell Hanford Operations, and the University of Washington. The USGS deployed a 260km-long line running NE-SW through the central basin with dense station spacing. The University of Washington set up unreversed refraction lines with sparse station spacing concentrated to the west of the USGS line while Rockwell Hanford Operations deployed stations to the east. Starting with the dense data from the reversed USGS line, intercept times and crossover distances were used to create a two-layered model. This model was then expanded to five layers, including a low-velocity layer beneath the basalts, by using an iterative scheme of two-dimensional forward ray-tracing and data from several deep boreholes.

The model consists of a 0.5km-thick, 3.7km/s surface layer overlaying the basalts, which have an average velocity of 5.18km/s. The average velocity for the low-velocity layer ranges from 4.6km/s to 5.0km/s. Deep borehole sonic logs confirm the existence of this low-velocity layer and are used to fix the depth to the bottom of the basalts in the northern region. Analysis of the refraction data reveals that the basalts extend to a depth of approximately 5.4km in the central basin and thin to a depth of 1.8km in the northeast and 0.8km in the northwest. The top of the 6.2km/s crystalline basement refractor extends to depths between 10km and 11km in the central basin and shallows to the north. Shallowing of the basement rock was confirmed by additional refraction data collected from a local mine in the northern part of the study area. A deep-crustal layer with an average velocity of 7.2km/s begins at depths of about 18km in the south increasing to approximately 22km in the northern part of the study area.

TABLE OF CONTENTS

LIST OF FIGURES

LIST OF TABLES

ACKNOWLEDGMENTS

I am sincerely grateful to my adviser, Stephen D. Malone, for his helpful suggestions and constructive criticism. Also, I thank Al Rohay for providing some instruments used in the experiment and access to all the data collected for the Basalt Waste Isolation Project of Rockwell Hanford Operations. Al has contributed enormously to the analysis through our numerous discussions on the region. I am also grateful to Walter Mooney and Rufus Catchings who taught me a great deal about the interpretation of seismic refraction data and who supplied me with the USGS record sections. This research was supported by grants from the U.S. Department of Energy (EY-76-S-06-2225) and the U.S. Nuclear Regulatory Commission (NRC-04-81-177).

I am indebted to the many who worked in the field during this experiment: Jim Hudspeth, Scott Key, Eric Lanning, Rob Leet, Steve Malone, Dawn Mullen, Bob Norris, Chris Trisler, Tom Yelin, and Jim Zollweg. This group worked long hours and their help is greatly appreciated. Thanks are due to Rick Benson and Charles Camisa for invaluable assistance with computer problems. I also thank Julie Shemeta and Rick Benson for their critique of my first practice talks on the results of the study.

I am grateful to Dave Boness, with whom I have had many helpful discussions both professionally and socially and to Opus who always provided a chuckle when I needed one most. I am especially grateful to Amy Handler who provided support throughout this project. Amy helped immensely with the editing of this thesis. Last, but far from least, I thank my parents. They have given me encouragement, unequaled support, and, most of all, love.

Chapter I -- INTRODUCTION

The Columbia Basin in eastern Washington is covered by a large field of flood basalts, yet proof is lacking about what lies beneath. No significant windows have been eroded through the basalts, thus preventing a definitive solution (McKee, 1972). Magnetotelluric data suggests that a rock low resistivity may exist beneath the basalts (Stanley, 1984). Stanley constructed a cross-section with a conductive sedimentary layer beneath a more resistive layer of basalt. Deep boreholes also provide clues on a local basis for the rock type beneath the basalts. In the northern part of the region deep boreholes cut through the basalts into sediments (Lewis, 1982; Campbell, in preparation (a)). However, the magnetotelluric data and the deep boreholes do not provide details of the existence of this sedimentary layer throughout the entire region.

In August, 1984 the U.S. Geological Survey (USGS), in conjunction with the Basalt Waste Isolation Project of Rockwell Hanford Operations (BWIP-RHO), and the University of Washington, conducted a large-scale seismic refraction experiment in eastern Washington. Data were collected from four different shot points during this experiment. Data were also collected from several blasts from a local mine in the area. Refraction lines splayed out in different azimuths from the shot points, frequently crossing other refraction lines along the way. These refraction lines provided good coverage of the study area. A two-dimensional model was created along each refraction line. Where the lines intersected, the depth to each layer in the model was tied together. Hence, a three-dimensional model for the entire study area was

created by considering all of the two-dimensional models.

Project Goals

Figure 1.1 is an index map of the Pacific Northwest. The bold outline on the map marks the boundary of the study area for the experiment. In the heart of the study area is the U.S. Government's Hanford Reservation. This is one of three sites chosen for the possibility of housing the nation's first commercial high-level nuclear waste repository. The three sites are undergoing further investigation. The proposed repository, if Hanford is chosen, would be built in basalt at a depth of about one kilometer. An issue as important as the construction of a nuclear waste repository demands an intimate knowledge of the geology and tectonic behavior of the region. Hopefully, the information determined from this experiment will aid in the understanding of the area. The emphases of the seismic refraction experiment are to determine the depth to the bottom of the basalt, to verify the existence of low-velocity sediments beneath the basalt, to determine the depth to the crystalline basement, and to extend the detailed work from the USGS line throughout the study area.

Investigation Method

For the purpose of this study, seismic refraction methods prove to be superior to reflection methods. Oil companies exploring in eastern Washington have had considerable difficulty with the waves scattering off the flow top breccias; thus, very little seismic energy penetrates through the basalts (Shirley, 1984). This has made the analysis of the structure beneath the basalts nearly impossible. The refraction method is chosen because the length of the lines enables the recording of refracted arrivals and wide angle reflections

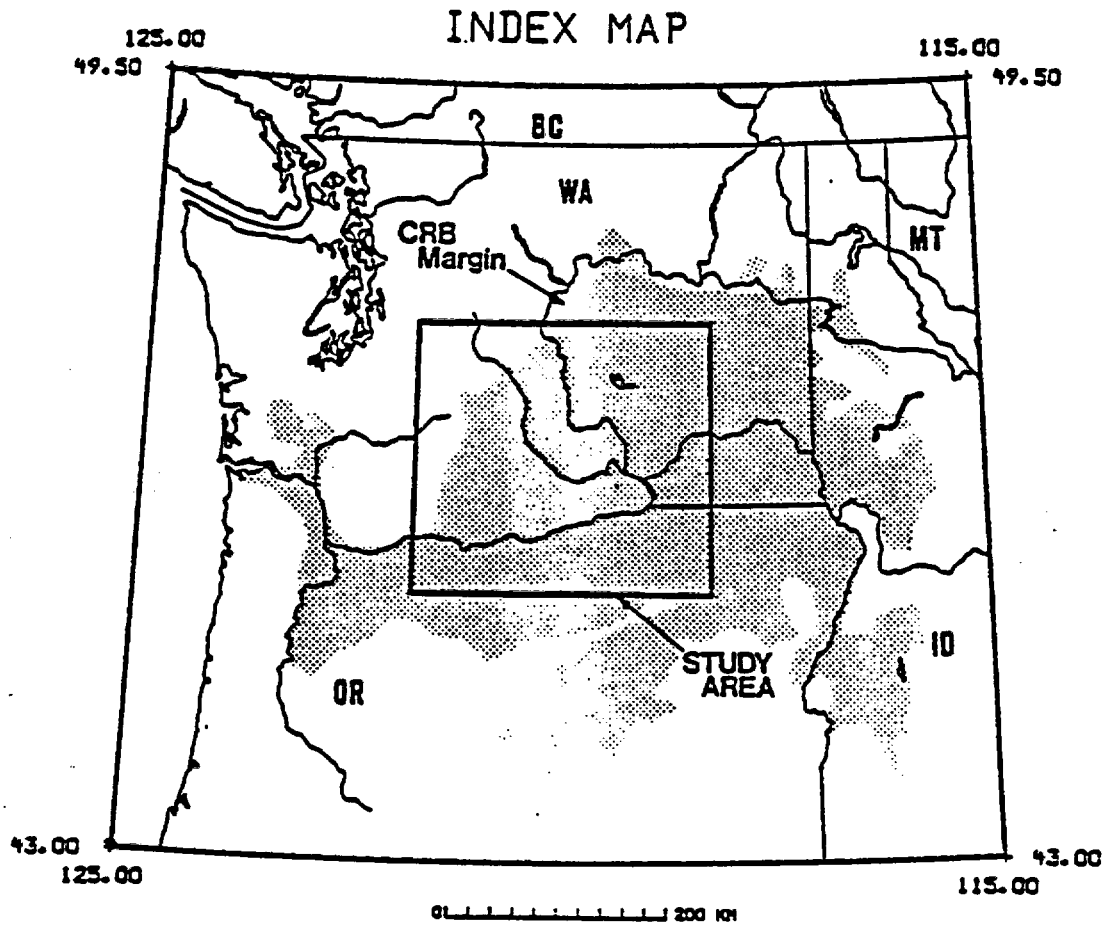

Figure 1.1 Index map of the Pacific Northwest. Bold outline encloses the study area and the stippled region denotes the Columbia River Basalt Group (basalt area from Myers et al., 1979).

from layers beneath the basalts. Refraction data also provides evidence of low-velocity layers in the crust. This evidence is seen on the records as shadow zones and greater delay times between refractors. In addition to the refraction data, information from four deep boreholes in the northern part of the study area have been used to aid in the analysis of the crustal structure.

Principal Results

A generalized model along the USGS line depicting five crustal layers has been derived independent of the USGS analysis (Catchings and Mooney, 1985). The main reason for the generalized interpretation of the USGS line is to use this crustal model and the borehole data to help derive models for the sparser data from the other refraction lines in the study area. Well logs from the deep boreholes have provided control on the depth to the bottom of the basalt in the northern part of the study area.

Through the use of two-dimensional forward ray-tracing (Cerveny, Molotkov, and Psencik, 1977) and borehole information, a model has been constructed with a low-velocity layer beneath the basalts. A computer program, written by Cerveny et al. and modified slightly by the USGS and the University of Washington, traces rays through laterally varying isotropic layers. This program approximates head waves by diving rays through layers with slight vertical velocity gradients.

A total of thirteen different interacting refraction lines have been analyzed, thus giving essentially a three-dimensional crustal model for the study area. Velocities determined from sonic logs from two deep boreholes substantiate the existence of a low-velocity layer and fix the depth to the bottom of the basalts in the northern area. The model consists of five layers – three layers on top of basement rock and a deeper crustal layer. A 0.5km-

thick surface layer with an average velocity of 3.7km/s has been used. The second layer is the basalts of the Columbia River Basalt group. An average velocity for the basalts is 5.18km/s. The bottom of the basalts extends to depths greater than 5.0km in the central part of the study area and then shoals to about 1.8km in the northeast and 0.8km in the northwest. The average velocity for the low-velocity layer is inferred to be approximately 4.7km/s. The depth to the crystalline basement is between 10.0km and 11.0km in the central part of the area and shallows to 3.9km in the northeast and 1.5km in the northwest. The crystalline basement has a velocity of approximately 6.2km/s. The deep crustal layer is between 18.0km and 23.5km throughout the study area. This layer is shallower in the south. The deep crustal refractor has an average velocity of 7.2km/s.

Chapter II -- REGIONAL GEOLOGY

Myers and Price, et al. (1979) have compiled an extensive list of references on the geology of the region for the Basalt Waste Isolation Project of Rockwell Hanford Operations. Much of this research was conducted by Rockwell Hanford Operations or by contractors for Rockwell. A summary of part of their work as well as that of a few other authors are included in this chapter.

Columbia River Basalt Group

The Columbia River Basalt Group (CRB) underlies most of the surface throughout the study area. The stippled region in Figure 1.1 shows the areal distribution of the CRB. The CRB is a field of flood basalts covering an area of approximately 200,000 square kilometers. These basalts erupted from north-northwest-trending linear fissures now preserved as dikes (Swanson, Wright, and Helz. 1975). The CRB is composed of tens to hundreds of individual flows deposited during the Miocene epoch (6.0 to 16.5 million years before present). Thin sedimentary rock layers exist between many of the basalt flows. An average thickness for a basalt flow is about 34 meters.

Five different formations comprise the CRB. From oldest to youngest they are the following:

Imnaha Basalt
Picture Gorge Basalt
Grande Ronde Basalt
Wanapum Basalt

Saddle Mountains Basalt

The Imnaha Basalt outcrops in northeastern Oregon, southeastern Washington, and southwestern Idaho. Outcrops of the Picture Gorge Basalt are located out of the study area in north-central Oregon. Most, if not all of the Picture Gorge Basalt is younger than the Imnaha Basalt and part of the Picture Gorge Basalt is coeval with the Grande Ronde Basalt. The Grande Ronde Basalt was deposited 14.0 to 16.5 million years before present. This extensive formation covers the largest area and comprises nearly 85% in volume of the CRB. The Grande Ronde Basalt is overlain by the Wanapum Basalt. The Wanapum Basalt is the second most voluminous formation of the CRB. On top of the Wanapum Basalt lies the Saddle Mountains Basalt, the youngest member of the CRB, having been deposited 6.0 to 13.5 million years before present. This formation comprises less than one percent of the total volume of the CRB.

Each formation of the CRB consists of several layers. These layers can be seen on sonic logs from boreholes through the basalt. The interbedded sedimentary rocks have much lower seismic velocities than the basalts. This difference can be seen quite easily on a velocity versus depth curve which is read directly from a sonic log (two examples of this are illustrated in Chapter 4). These layers can be seen on sonic logs, however; on a large-scale seismic refraction experiment only gross structure can be resolved. Thus for modeling the refraction data, the CRB can be interpreted as one layer with an average velocity which is influenced by the many thinner layers.

Tertiary Sediments

North of the study area Tertiary sedimentary rocks of the early Eocene Swauk Formation, late Eocene Chumstick Formation, and Oligocene Wenatchee Formation are known to exist (Gresens, 1983; Gresens and

Stewart, 1981; Gresens, Naeser, and Whetten, 1981; Tabor et al., 1984). The southward extent of the Tertiary sediments beneath the CRB is presently unknown. Gresens and Stewart (1981) and Gresens et al. (1981) hypothesize that Wenatchee type rocks may extend far to the south beneath the basalts. Campbell (in preparation (a,b)) suggests that the Chumstick Formation and the Wenatchee Formation could extend beneath the basalt toward the center of the Columbia Basin. Campbell (in preparation (a)) also states that Cretaceous marine sediments found in the Shell 1-29 Bissa Well could extend to the center of the basin.

Crystalline Basement

The crystalline basement just north of the study area is the Swakane Biotite Gneiss (Gresens et al., 1981). Schists and plutonic complexes are also present to the north and Campbell (in preparation (a)) states that the Shell 1-29 Bissa Well bottoms in granite. East of the study area the basement is Precambrian metasedimentary rocks of the Northern Rocky Mountains province and Mesozoic intrusive units of the Idaho Batholith province. To the south, the basement consists of Mesozoic to early Tertiary metamorphic rocks of the Blue Mountains subprovince.

Regional Structure

Several anticlinal structures are prominent topographic features within the study area. Figure 2.1 shows the major ridges in this area. The general trend of these ridges is northwest-southeast to almost due east-west. A description of the structures in the study area follows.

Manastash Ridge, one of the furthest north ridges in the study area, is a 55km-long structure which extends northwest from Badger Gap to just west

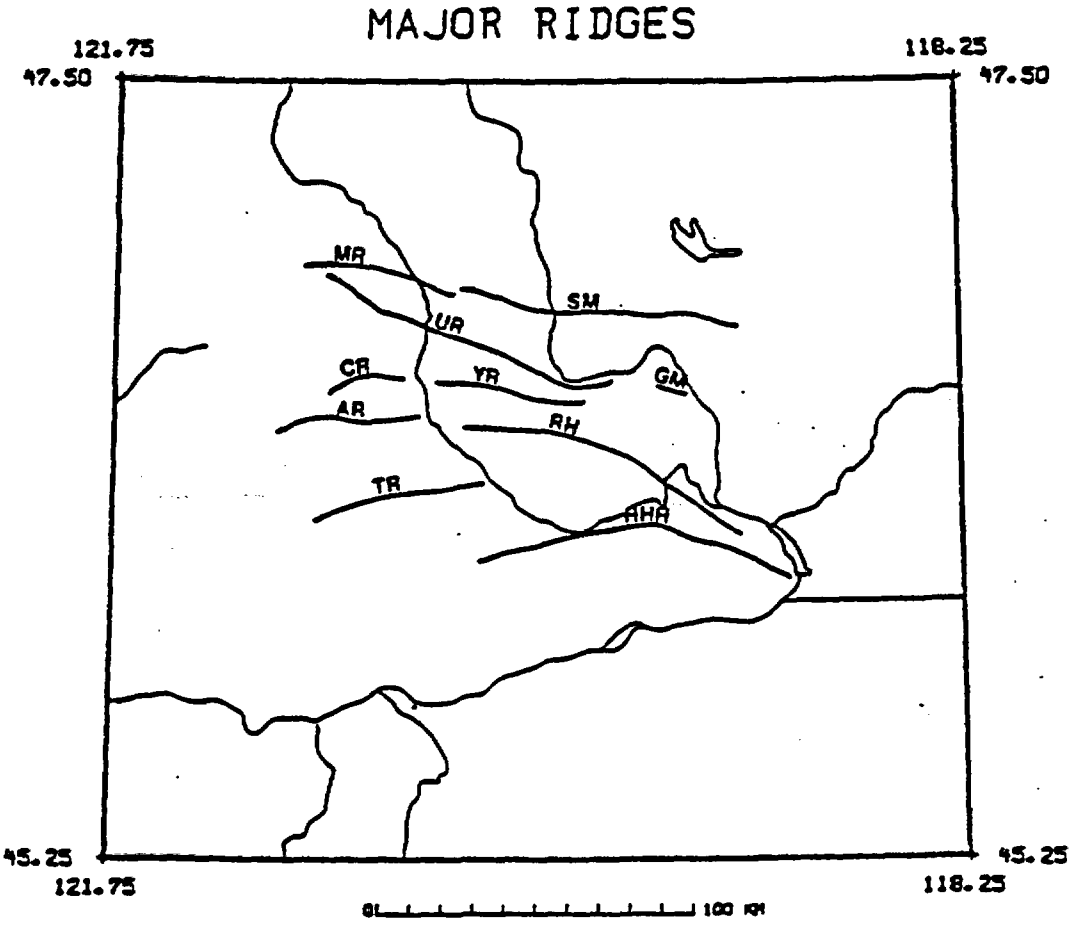

Figure 2.1 Map of the study area displaying the major ridges: MR (Manastash Ridge), SM (Saddle Mountains), UR (Umtanum Ridge), GM (Gable Mountain), CR (Cowiche Ridge), YR (Yakima Ridge), AR (Ahtanum Ridge), RH (Rattlesnake Hills), TR (Toppenish Ridge), and HHH (Horse Heaven Hills).

of Shushuskan Canyon, where it assumes a more east-west trend along the south fork of Manastash Creek (Myers et al., 1979). This ridge is an asymmetrical anticlinal structure which has steeper dipping beds on the northern limb (Smith, 1903).

The eastward extension of Manastash Ridge is the Saddle Mountains. The Saddle Mountains structure extends approximately 110km across the western portion of the Columbia Plateau (Myers et al., 1979). According to Russell (1893), this structure is a well-defined monoclinal ridge, tilted southward with a steep north face. The northern limb is overturned along parts of this ridge (Laval, 1956). Laval (1956) also states that this structure is actually an anticline that resembles a monocline. Myers et al. (1979) agree with this interpretation stating further that the main structure is an asymmetric anticlinal ridge with a steep northern flank.

The next major feature just south of the Manastash Ridge-Saddle Mountains structure is the Umtanum Ridge-Gable Mountain structure which extends a total of 110km (Myers et al., 1979). Gable Mountain and Gable Butte are currently interpreted as continuations of Umtanum Ridge because of their similar trends (Myers et al., 1979). Umtanum Ridge is an asymmetrical anticline with steep northern dips (Smith, 1903). Goff and Myers (1978) classify the Umtanum Ridge segment further as an asymmetric, noncylindrical, overturned, plunging anticline. Myers et al. (1979) also state that Gable Mountain and Gable Butte are topographically isolated anticlinal ridges of basalt and interbedded sediments.

South of Umtanum Ridge lie the Cowiche Ridge-Yakima Ridge complex. Waters (1955) states that Yakima Ridge is a less continuous anticline than most of the other ridges. Yakima Ridge and its western continuation, Cowiche Ridge, are about 100km long (Waters, 1955).

Ahtanum Ridge is the next major topographic feature heading further south. Myers et al. (1979) state that Ahtanum Ridge is an asymmetrical anticline trending east-west and extending approximately 32km. The Rattlesnake Hills anticline is the eastern extension of Ahtanum Ridge. Laval (1956) points out that the southeastern end of the Rattlesnake Hills merges with the Horse Heaven Hills structure.

Toppenish Ridge, south of Ahtanum Ridge, is a 125km-long anticlinal ridge located in the southwestern part of the study area (Myers et al., 1979). Laval (1956) states that Toppenish Ridge is a composite anticline formed in a broad arch with subsidiary anticlinal flexures.

The major structure furthest south in the study area is the Horse Heaven Hills. This anticline flanks the northern edge of the Horse Heaven Plateau (Laval. 1956).

Several of the refraction lines interpreted from this experiment crossed one or more of the ridges. An elevation correction was not used for stations placed on these ridges nor was the topography modeled in the two-dimensional cross sections. However, a 0.5km-thick surface layer with a 3.7km/s average seismic velocity was used. The major composition of these ridges is basalt and the deposition of sediments has been confined mainly to the plateau areas between the ridges (Myers et al., 1979). This surface layer not only models the sediments between the ridges well, but also compensates for the additional distance the seismic waves travel when going through a ridge. The relief difference along a refraction line that intersects a ridge is generally on the order of 0.3km to 0.4km. The time difference for waves traveling through 0.5km of sediment at 3.7km/s and 0.85km of basalt (this gives a height of 0.35km for the ridge) at 5.18km/s is only 0.03s which is within the picking error of the first arrivals for most of the stations.

Therefore, the use of a constant-thickness surface layer is a valid approximation for the surface topography in the study area.

Chapter III -- DATA ACQUISITION AND ANALYSIS

In August, 1984 the USGS, the Basalt Waste Isolation Project of Rockwell Hanford Operations, and the University of Washington collected data from a large-scale seismic refraction experiment in eastern Washington. The data from each of the three groups were used in the analysis presented in this thesis.

U.S. Geological Survey

The USGS detonated eight blasts at four different locations -- one at each location on two separate nights. The first night shot #1 was a large blast while shot #'s 2, 3, and 4 were about half the size. On the second night shot #4 was a large blast while the other three blasts were about half the size. These blasts ranged in size from 900kg to 2300kg. The blast locations are given in Table III.1. The blast location from the Cannon Mine, which will be discussed later, is included as well.

TABLE III.1 Blast Sites

Name	Latitude	Longitude
Shot #1	46°58.24′	119°51.73′
Shot #2	46°40.57′	119°27.97′
Shot #3	46°20.88′	119°50.30′
Shot #4	45°56.45′	120°84.77′
Cannon Mine	47°23.27′	120°20.27′

The USGS set up a 260km-long refraction line that ran between the blasts and extended 60km past shot #1 and shot #4. Figure 3.1 is a map of the study area showing the USGS refraction line. The squares on the map represent the shot points and the triangles represent the seismic stations and deep boreholes.

The USGS data were recorded by 120 portable instruments on FM analog tapes which were later digitized (Healy et al., 1982). These instruments were deployed on each night so that a total of 240 sites were occupied. The USGS used a 0.9km station spacing between the shots and a 1.3km station spacing northeast of shot #1 and southwest of shot #4. This dense station spacing was used to obtain high resolution for the crustal models.

Rockwell Hanford Operations

The Basalt Waste Isolation Project of Rockwell Hanford Operations runs a permanent seismic network in the center of the study area. They also set up a temporary network consisting of thirteen stations just east of the USGS deployment. BWIP-RHO operated two types of portable instruments in their temporary network – Sprengnether MEQ-800 portable drum recorders and Sprengnether DR-100 portable digital recorders. These instruments were deployed in a fairly even spacing to provide sufficient coverage for an analysis of the data using a time term method. Table III.2 is a list of the locations and the blasts recorded by their temporary stations.

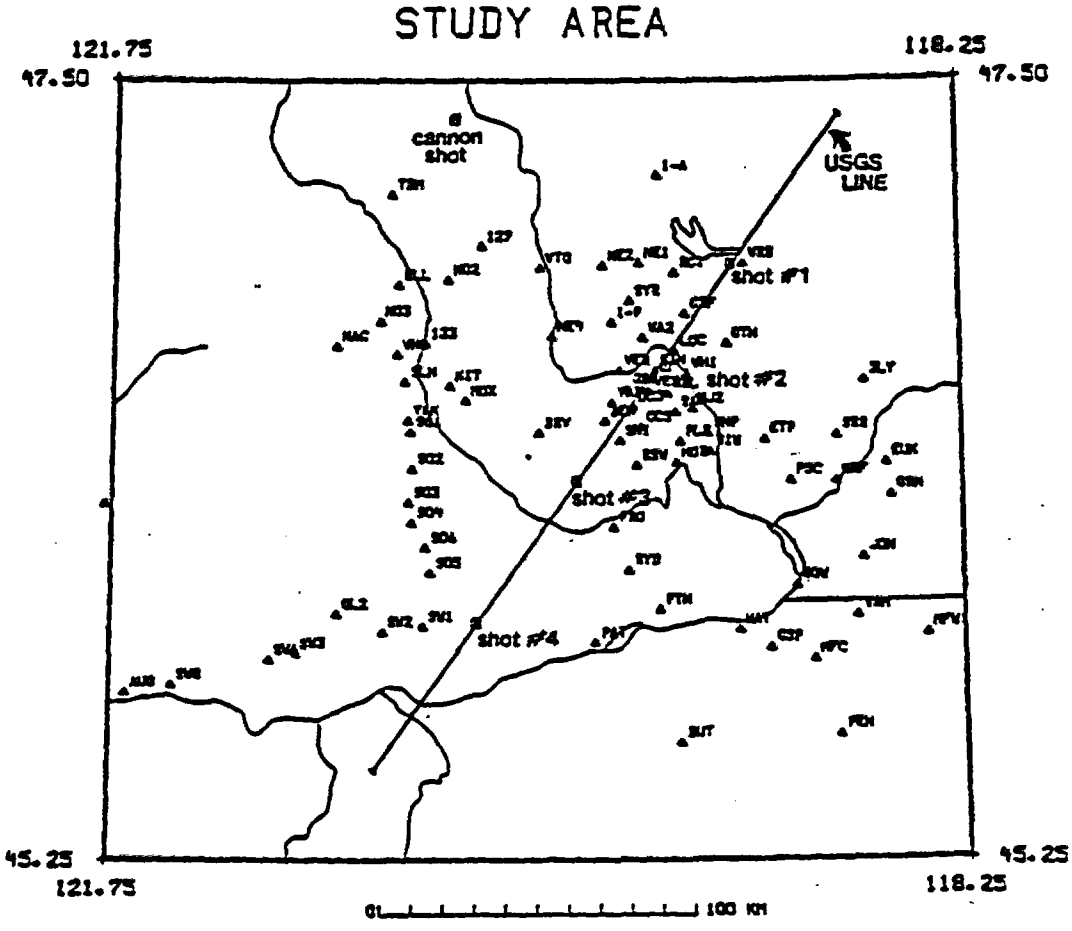

Figure 3.1 Map of the study area for the experiment is shown with the USGS line. Squares indicate shot points and triangles are seismic stations and deep boreholes.

TABLE III.2 BWIP-RHO Temporary Network

Name	Latitude	Longitude	Shot #'s recorded
RYD	46°05.35′	119°37.32′	2,3,4
PTN	45°58.52′	119°29.80′	2,3,4
HAT	45°55.05′	119°10.20′	2,4
BUT	45°35.43′	119°24.78′	1,2,3,4
CSP	45°51.97′	119°02.37′	1,2,4
MFC	45°49.93′	118°51.75′	1,2,3,4
WRM	45°57.40′	118°41.15′	1,2,4
JON	46°07.42′	118°39.57′	1,2,4
GRN	46°18.08′	118°32.72′	1,2,3,4
MUR	46°20.67′	118°46.05′	1
SRR	46°28.57′	118°45.78′	1,2,3,4
DLY	46°37.90′	118°39.05′	1,2,3,4
PSC	46°20.73′	118°57.18′	2

University of Washington

The University of Washington operated five kinds of seismic recorders for the USGS experiment; four of the recorders were portable. The non-portable instruments are used for the permanent seismic network operated by the University of Washington. The stations in the permanent network are telemetered directly to an on-line computer system at the university. Three temporary stations, WNS, SLH, and KIT, were telemetered to the on-line system as well. The portable instruments included strip chart recorders, Sprengnether DR-100 recorders, Sprengnether MEQ-800 recorders, and Terra Technology DCS-302 recorders. The data from the Sprengnether DR-100 portable digital instruments were recorded on high quality cassette tapes. A program was written to convert this data into the same format as the data from the stations in the University of Washington's permanent seismic network. The trace data from the stations using the DR-100's could then be

plotted on record sections along with data from the permanent stations. The data from the strip chart recorders and the MEQ-800 portable drum recorders were not digitized, so only first arrivals could be plotted on the record sections. The data obtained from the DCS-302 portable digital recorders were not merged with the other trace data, so again, only first arrivals could be plotted on the record sections. Figure 3.2 shows a typical record section along one of the refraction lines from the experiment. The circles indicate first arrivals from portable instruments.

The University of Washington set up several refraction lines directed away from the USGS shot points. Temporary stations, coordinated with the locations of the permanent stations, were set up along these unreversed lines. The data from all the refraction lines interpreted in this study, except the USGS line, are included in Appendix I. The permanent stations involved in the planning of the refraction lines were VTG, ELL, TBM, NAC, YAK, SYR, BRV, GL2, and AUG. AUG, however, did not supply any useable data because of excessive noise. Nineteen stations set up for the temporary network recorded useable data. The temporary stations operated by the University of Washington are listed in Table III.3.

The on-line system triggered for seven of the eight blasts. The system did not trigger for shot #4 on the first night; however, it did trigger the second night when shot #4 was the large blast. Therefore, data from all four of the shot points were recorded by stations telemetered directly to the university.

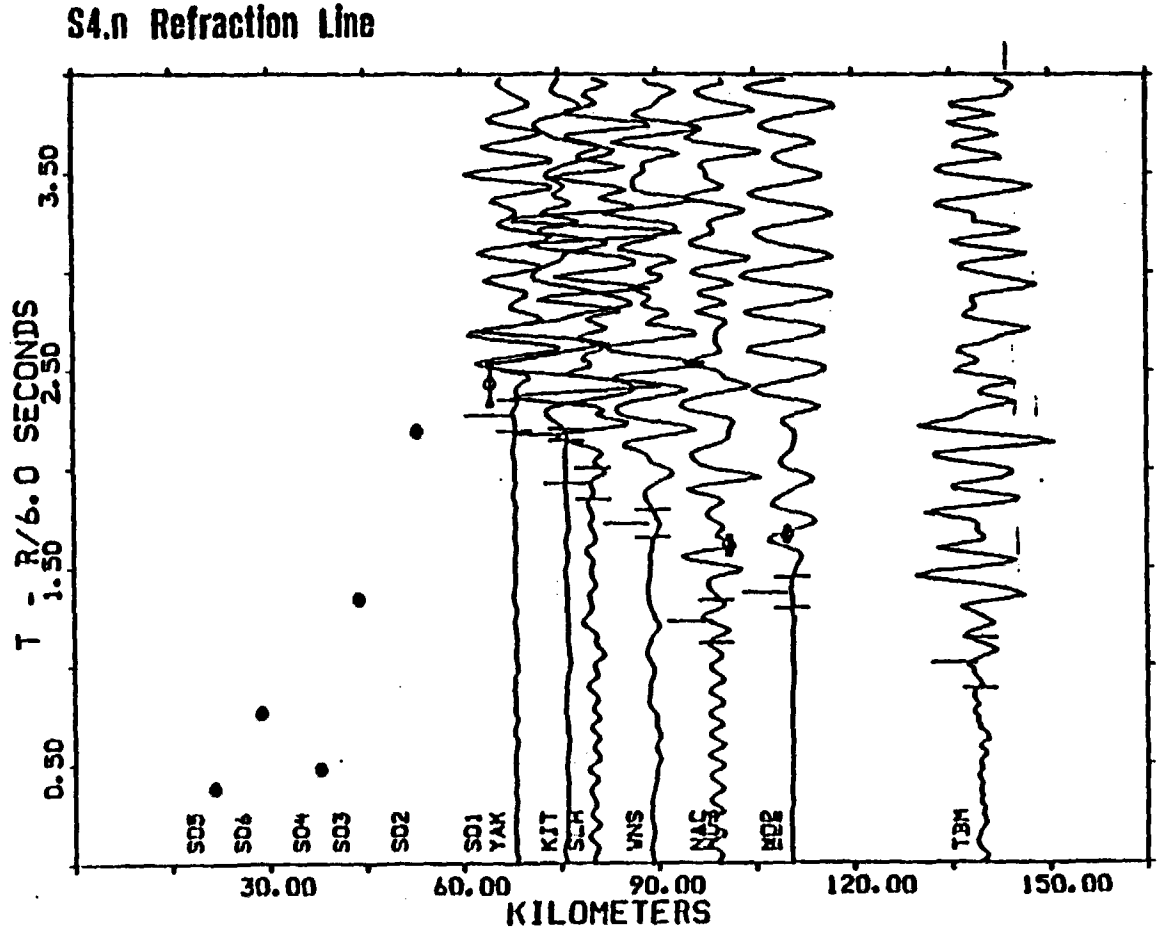

Figure 3.2 Record section showing data along the S4.n refraction line -- reduced traveltimes are plotted. First arrival times from the portable drum recorders are displayed as circles.

TABLE III.3 University of Washington Temporary Network

Name	Latitude	Longitude	Shot #'s recorded
NE1	46°58.35′	119°34.68′	1,2
NE2	46°57.93′	119°43.70′	1
NE4	46°45.70′	119°56.27′	1
N02	46°55.50′	120°21.97′	2,4
N03	46°48.32′	120°38.80′	1,3,4
WNS	46°42.62′	120°34.50′	1,2.3,4
SLH	46°37.92′	120°32.47′	1.2.3,4
KIT	46°37.22′	120°21.42′	1,2.3,4
S01	46°29.30′	120°31.07′	4
S02	46°22.93′	120°30.63′	1.2.3,4
S03	46°17.10′	120°31.60′	1.2.3,4
S04	46°13.60′	120°30.75′	1.2.3.4
S06	46°09.28′	120°27.33′	1.2.3,4
S05	46°04.95′	120°26.15′	1.2.3.4
SW1	45°55.67′	120°27.93′	1.2.4
SW2	45°54.70′	120°37.92′	1.2.4
SW3	45°51.00′	120°59.33′	2.3.4
SW6	45°49.93′	121°05.75′	2.3.4
SW8	45°45.50′	121°29.62′	2.4

Data from eight blasts from the Cannon Mine near Wenatchee were also collected for this study. These blasts were recorded on the stations in the permanent network over a period of nine months from October, 1984 to June, 1985. An MEQ-800 portable drum recorder was set up 1.1km from the source for one of the eight blasts. An origin time for this one blast was then closely approximated by assuming a 3.7km/s surface layer -- the same surface layer velocity used in the two-dimensional models introduced later. The origin times for the other seven blasts were estimated by comparing first arrival times to several stations with those from the blast with the known origin time. To minimize the first arrival picking error, average times were used as the data from the Cannon Mine.

Deep Boreholes

Four deep boreholes used in this study are located in the northern part of the area. These wells are the following: the Snowbird Resources 1-A Moses Lake Well, the Shell 1-9 BN Saddle Mountains Well, the Shell 1-29 Bissa Well, and the Shell 1-33 Yakima Minerals Well. The locations of these wells are listed in Table III.4.

TABLE III.4 Well Locations

Name	Latitude	Longitude
1-A	47°13.40′	119°30.00′
1-9	46°48.10′	119°41.60′
129	47°01.30′	120°13.70′
133	46°44.50′	120°27.50′

Analysis Technique

Thirteen refraction lines were interpreted for this crustal structure study of eastern Washington. Figure 3.3 shows all of the lines that were analyzed. The USGS line was used along with twelve other lines with station spacing ranging from about 5km to 15km. These other refraction lines used stations from the University of Washington's and the BWIP-RHO's permanent and temporary networks. The refraction lines analyzed are the following: the USGS line, S1.w, S1.wsw, S2.s, S2.sse, S2.se, S3.nw, S3.e, S3.se, S4.n, S4.w, S4.e, C.s (the reversal of the northern part of S4.n), and C.sse. The naming convention for these lines is the shot point followed by the direction of the line.

The USGS set up instruments along a reversed refraction line with dense station spacing. Therefore this line was the first refraction line to be analyzed. The other refraction lines interpreted from this experiment had

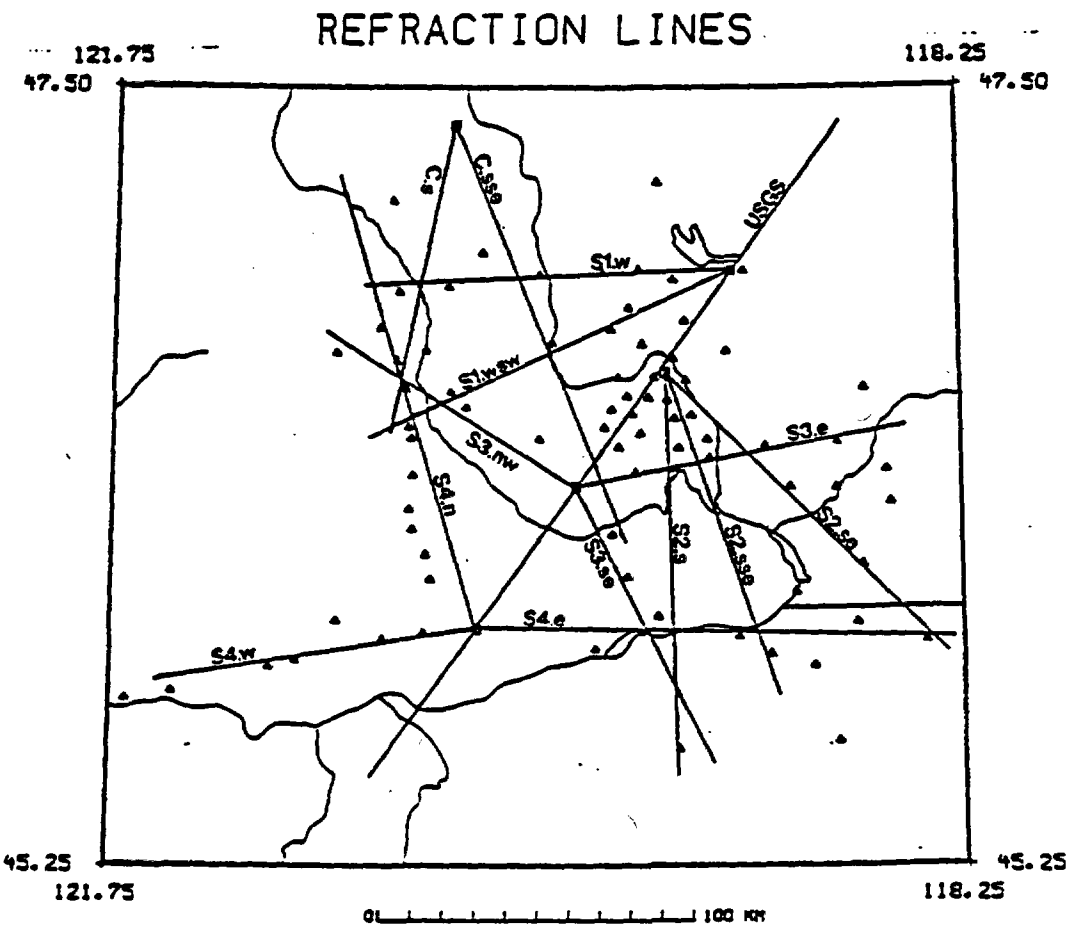

Figure 3.3 Map showing all the refraction lines that were analyzed in this study.

sparser station spacing and were not reversed (except for C.s). Using data from all four shot points along the USGS line, a simple two-layered model was created by using equations involving crossover distances and intercept times to calculate the depths to a dipping interface (Dobrin, 1976). A low-velocity layer was added by observing sonic logs from two boreholes and shadow zones present on some of the USGS record sections. Once a three-layered model for the USGS refraction line was determined, the data analysis was begun on the other refraction lines.

Refraction lines that ran near boreholes were the next to be analyzed. The starting models for these lines were based on the depths to each layer from the USGS line and layer depths determined from the boreholes. An iterative forward modeling scheme of two-dimensional ray-tracing was then implemented to adjust the models along the refraction lines. Through this method the depths to each layer were altered slightly to make the model arrival times match the real data arrival times. Since no major geologic faults are known to be located in the study area and since the station spacing was on the order of 10km, the interfaces between the layers in the models were made as smooth as possible. Refraction lines that did not have well control were interpreted with the same method. Next, the depths to each interface along a refraction line were tied together with the crossing refraction line at the intersection point.

A surface layer was added to the model after the three-layered model was created. To compensate for this new layer the two-dimensional model for each line was modified slightly through iterative ray-tracing. Finally, first arrivals from stations greater than 100km from the source provided evidence for the existence of a deep crustal layer. Therefore the deep crustal layer -- the fifth layer -- was added to the models.

Chapter IV -- RESULTS

Well Log Data

Sonic logs from two wells in eastern Washington were obtained for velocity analyses. These wells are the Shell 1-29 Bissa Well and the Shell 1-33 Yakima Minerals Well. Information from well logs was also obtained for the Snowbird Resources 1-A Moses Lake Well and Shell 1-9 BN Saddle Mountains Well. The Snowbird Resources 1-A Moses Lake Well was still in basalt at a depth of 2.1km and the Shell 1-9 BN Saddle Mountains Well cut through the basalt at 3.5km and bottomed in sediments at 4.6km (Campbell, in preparation (a)).

The velocity analysis and stratigraphic interpretation for the Shell 1-29 Bissa Well and the Shell 1-33 Yakima Minerals Well are shown in Figure 4.1. The bold line superimposed on the sonic velocity versus depth curve indicates a reasonable estimate for the velocity model for the two-dimensional crustal models. The gradients were used to generate up-turning rays in each layer to approximate head waves. A 0.5km-thick surface layer is used in most of the study area. The 3.7km/s average velocity for this layer is based on data from shallow wells in the central basin (Rohay, personal communication). The second layer is the basalts of the CRB. In the Shell 1-29 Bissa Well, the basalts end at a depth of about 1.4km where the Tertiary sediments begin. In a typical cross-section, the velocity in the two-dimensional models for the basalts increases from 5.00km/s to 5.35km/s. The low-velocity Tertiary sediments have an increasing velocity with depth from about 4.0km/s to

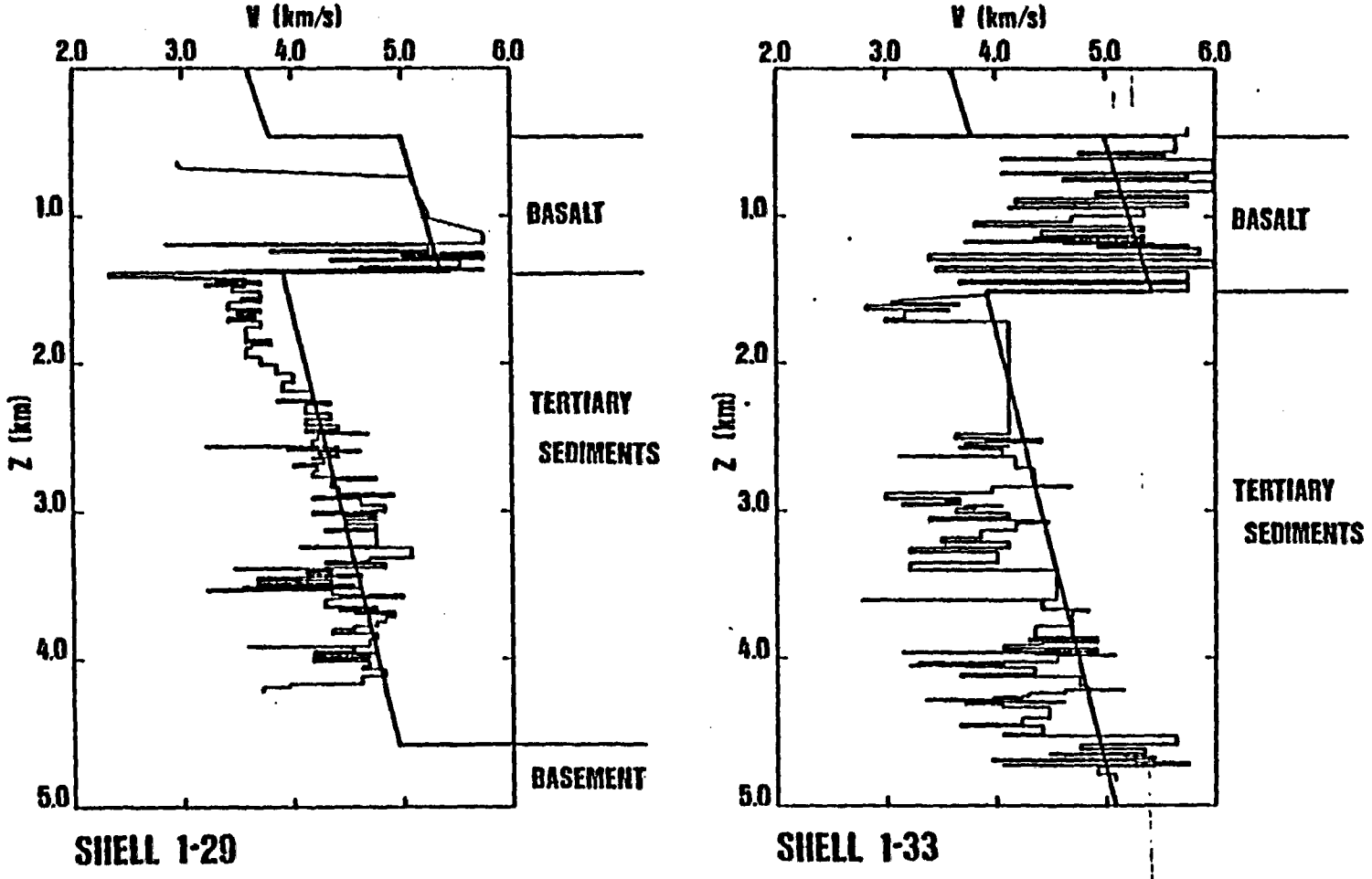

Figure 4.1 Sonic velocity vs. depth curves for the Shell 1-29 and 1-33 wells with two-dimensional ray-trace velocity models superimposed. Stratigraphic interpretation included on the right of each graph.

5.0km/s. I was only able to obtain the sonic log to a depth of about 4.2km for this well, however, Campbell (in preparation (a)) states that the well enters granite -- the basement rock -- at about 4.6km. The basalts bottom at a depth of about 1.5km in the Shell 1-33 Yakima Minerals Well. The sonic log, which ends at 4.8km, exhibits a velocity higher than 5.0km/s near the bottom of the well. These two wells have a very similar sonic velocity versus depth curve.

The Shell 1-29 Bissa Well, the Shell 1-33 Yakima Minerals Well, and the Shell 1-9 BN Saddle Mountains Well provided the depth to the bottom of the basalt in the northern part of the study area. These wells also helped place bounds on the velocities of the Tertiary sediments beneath the basalts. These data were used as a control for the two-dimensional models introduced in the following sections.

USGS Refraction Line

The USGS refraction line ran northeast-southwest through the Hanford Reservation. The line between shot #1 and shot #4 was reversed. The part of the line northeast of shot #1 and southwest of shot #4 was unreversed. The model along this line was based mainly on first arrivals and data from the well logs. Figure 4.2 and Figure 4.3 show the model and travel-time curves along this line. Circles on the travel-time curves indicate first arrival times for the real data read at 10.0km intervals from the USGS record sections. X's indicate arrival times for the model. The source in Figure 4.2 is shot #1 (located at 180.0km on the plot) and the source in Figure 4.3 is shot #4 (located at 40.0km on the plot). Shot #2 is located at about 141.0km on the cross-section and shot #3 is near 95.0km.

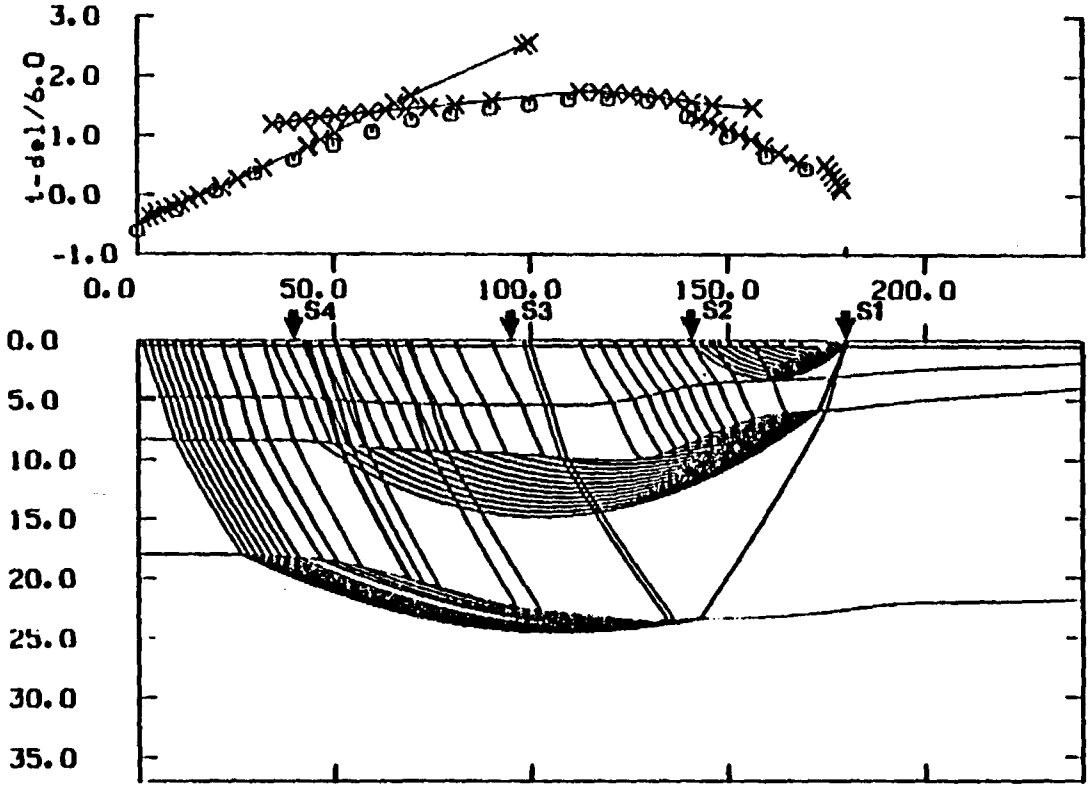

Figure 4.2 Two-dimensional ray-trace model for USGS.sw (USGS line from shot #1). In the upper portion of the figure the observed reduced traveltimes are shown as open circles and the calculated reduced traveltimes, obtained by ray-tracing, are shown as x's.

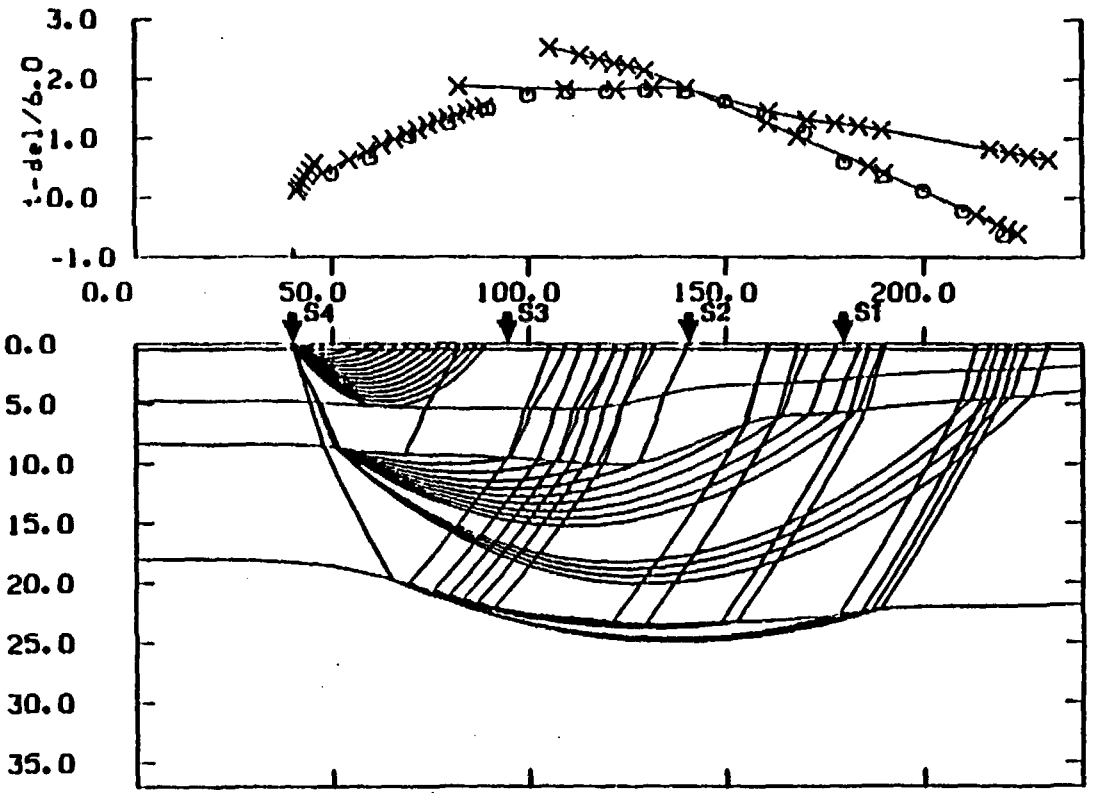

Figure 4.3 Two-dimensional ray-trace model for USGS.ne (USGS line from shot #4). Presentation as in Figure 4.2.

The model consists of five layers. In this simplified model of the earth's crust the surface layer is a constant 0.5km thick with an average velocity of 3.7km/s. The second layer is the Columbia River Basalt Group. The CRB is approximately 5km thick in the center of the basin, where it extends to a depth of 5.4km. At about 150km on the plot, the basalts in the model extend to a depth of 3.5km, which is the tie point with the Shell 1-9 BN Saddle Mountains Well. The basalts then thin toward the northern end of the model. Here the basalts extend to a depth of about 1.8km, hence, they are 1.3km thick. The velocity in this layer increases from 5.00km/s at the top of the layer to 5.20km/s at the bottom of the layer near shot #1 and to 5.40km/s at the bottom of the layer near the center of the basin.

Tertiary sediments comprise the third layer of the model. These sediments are 3.6km thick near shot #4, increase in thickness to 4.6km in the center of the basin, and thin again in the north to a 2.1km thickness. This layer has an average velocity lower than the basalts which makes observing refracted arrivals from this layer impossible. The average velocity in this layer varies from 4.6km/s to 5.0km/s. In the north, where the overlying rock is relatively thin, the velocity at the top of the layer is 4.1km/s and 5.0km/s at the bottom. Near the center of the model where the basalts are thickest, the overburden stress on the Tertiary sediments is greater. Therefore in this area, the velocity of the sedimentary layer increases with depth from 4.7km/s to 5.3km/s.

The crystalline basement rock, having an average velocity of 6.2km/s, lies beneath the Tertiary sediments. Near the center of this line the basement is at a depth of 10.0km and shallows in the north to 3.9km. Beneath the crystalline basement lies a 7.2km/s deep crustal layer. The top of this layer is at a depth of 18.3km underneath shot #4, 23.5km beneath the center

of the basin, and then shallows again in the north to about 22.0km. The bottom of the model is at 37.0km. This depth could possibly be near the crust-mantle boundary, however, the Moho depth in this area is not well constrained.

Shot #1 Refraction Lines

Two refraction lines using shot #1 as the source, S1.w and S1.wsw, are shown in Figure 4.4. Stations which provided data considered in the analysis lie in the stippled area on the map. The refraction lines were approximated as straight lines for the interpretation.

S1.w

The S1.w refraction line began at shot #1 and headed almost due west through the permanent network stations VTG and ELL. The model along this line is shown in Figure 4.5. This line intersected two other lines besides the USGS line at shot #1 – line C.sse at VTG, and also line S4.n (and C.s, the reversal of S4.n) at ELL. Thus, the depth to each layer has three tie points where the refraction lines intersect. Also, line S1.w passed just 10km south of the Shell 1-29 Bissa Well which enters the crystalline basement at a depth of 4.6km. This well provided evidence that the crystalline basement becomes shallower near the center of the line and then deepens again further west. The basalts thin to the west as the end of the line approaches the CRB margin. The deep crustal layer is included in the model because the arrival time at ELL (104km from the source) could be from either the crystalline basement or the deep crustal layer.

S1.wsw

The S1.wsw refraction line went through the permanent network stations SYR and YAK. The model for this line is shown in Figure 4.6. This

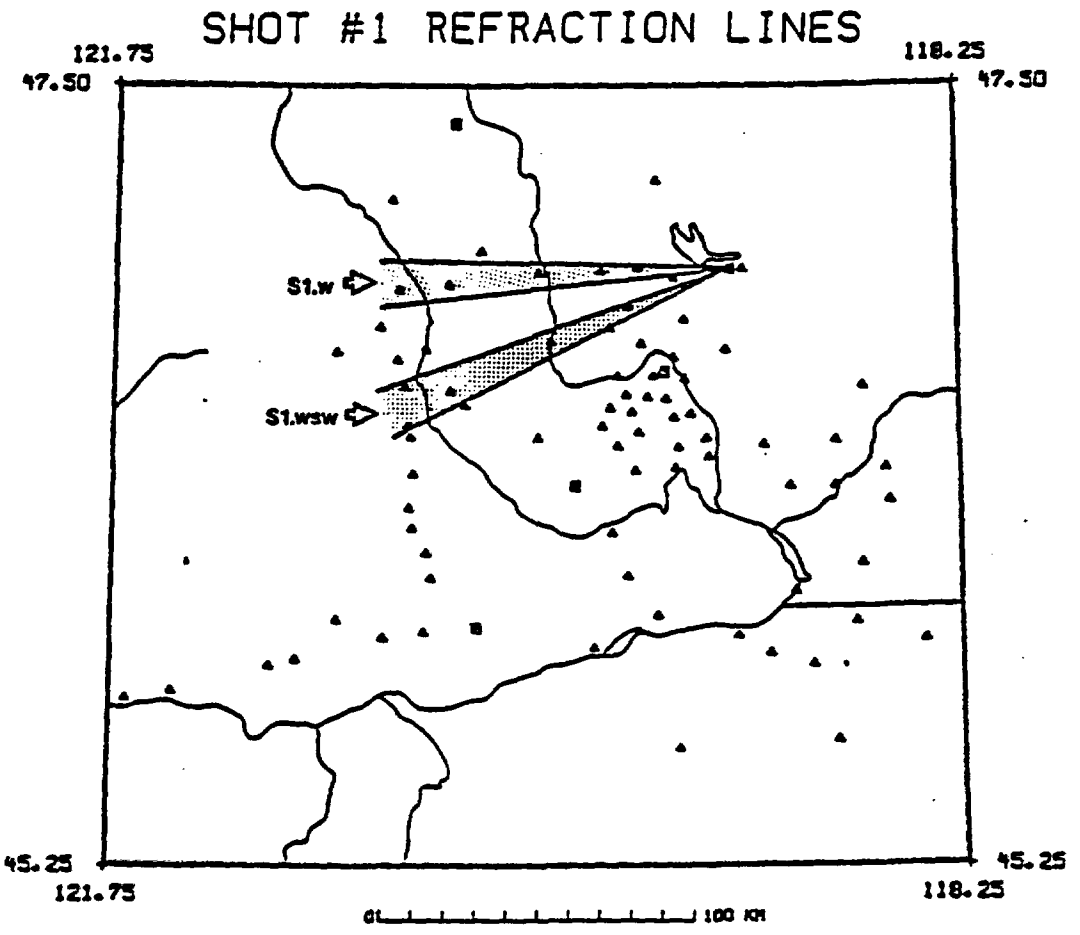

Figure 4.4 Map showing shot #1 refraction lines. Stations considered in the analysis are located in the stippled regions.

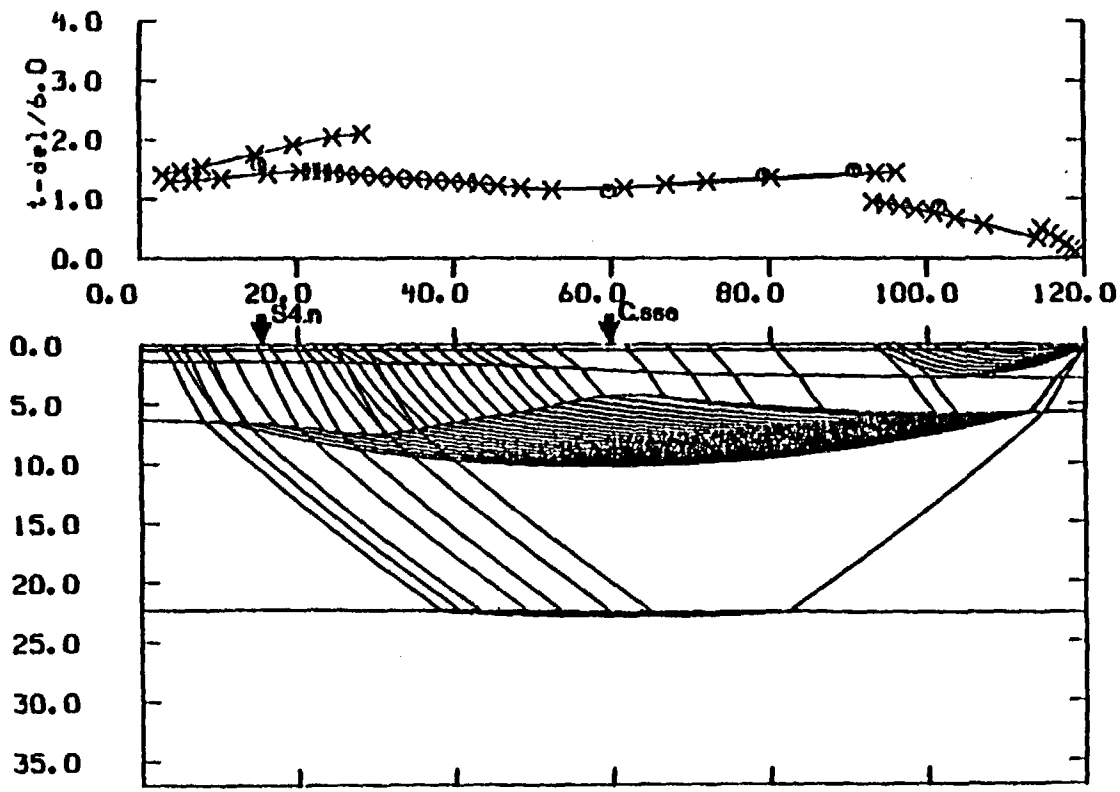

Figure 4.5 Two-dimensional ray-trace model for S1.w. Presentation as in Figure 4.2.

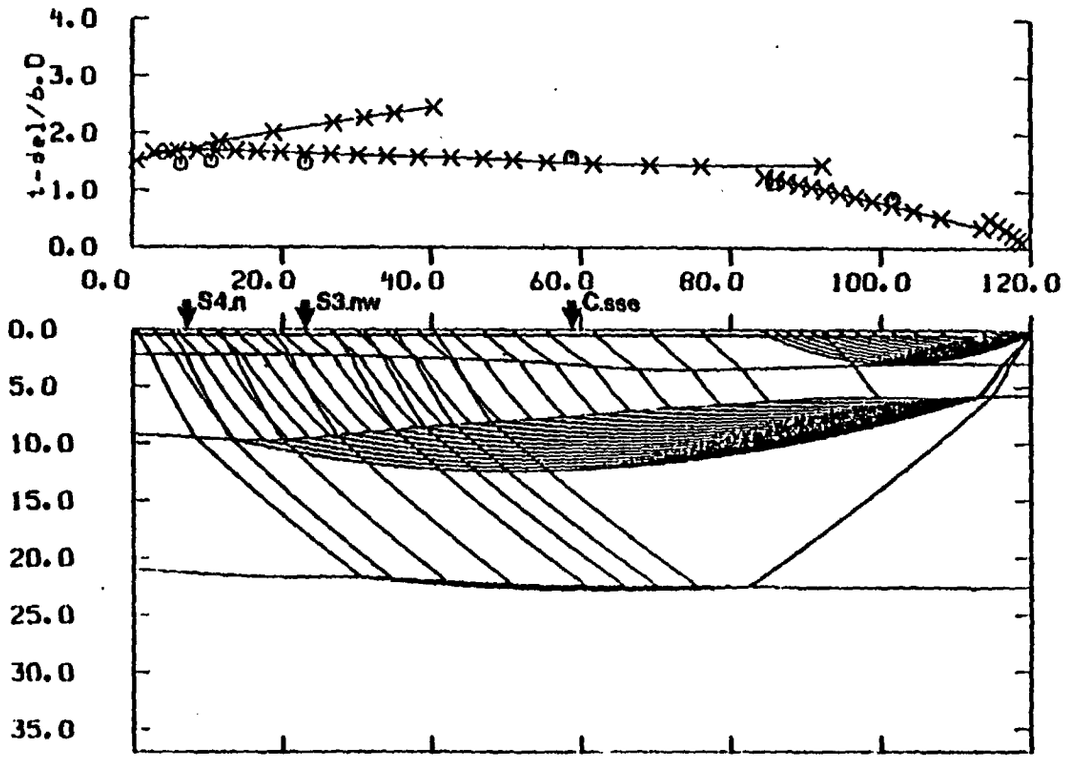

Figure 4.6 Two-dimensional ray-trace model for S1.wsw. Presentation as in Figure 4.2.

line intersected four other refraction lines: the USGS line at shot #1, line C.sse at NE4 (61.2km from the source), line S3.nw at KIT (96.8km from the source), and line S4.n near YAK (about 113km from the source). In addition to these tie points, the Shell 1-9 BN Saddle Mountains Well was located very close to this line about 42km from the shot point. This well provided control for the depth to the bottom of the basalt.

Shot #2 Refraction Lines

Three refraction lines beginning at shot #2 are shown in Figure 4.7. These lines are S2.s, S2.sse. and S2.se.

S2.s

The S2.s refraction line started from the USGS line at shot #2 and crossed both S3.e and S4.e. Figure 4.8 shows a model of the crustal structure along S2.s. The end of the line covered the same area as S3.se. For this part of the line, the model is identical with that of S3.se. Line S4.e provides a good tie point for the deep crustal refractor. Not much data exists from this layer further south, therefore the deep crustal refractor has been modeled as a flat layer south of S4.e.

S2.sse

The middle line originating at shot #2 is S2.sse. The model along this line is shown in Figure 4.9. Refraction line S2.sse intersected S3.e and S4.e. Because of the lack of data farther than 100km, no evidence exists for refractions from the deep crustal layer. Therefore, this layer has not been included in the cross-section.

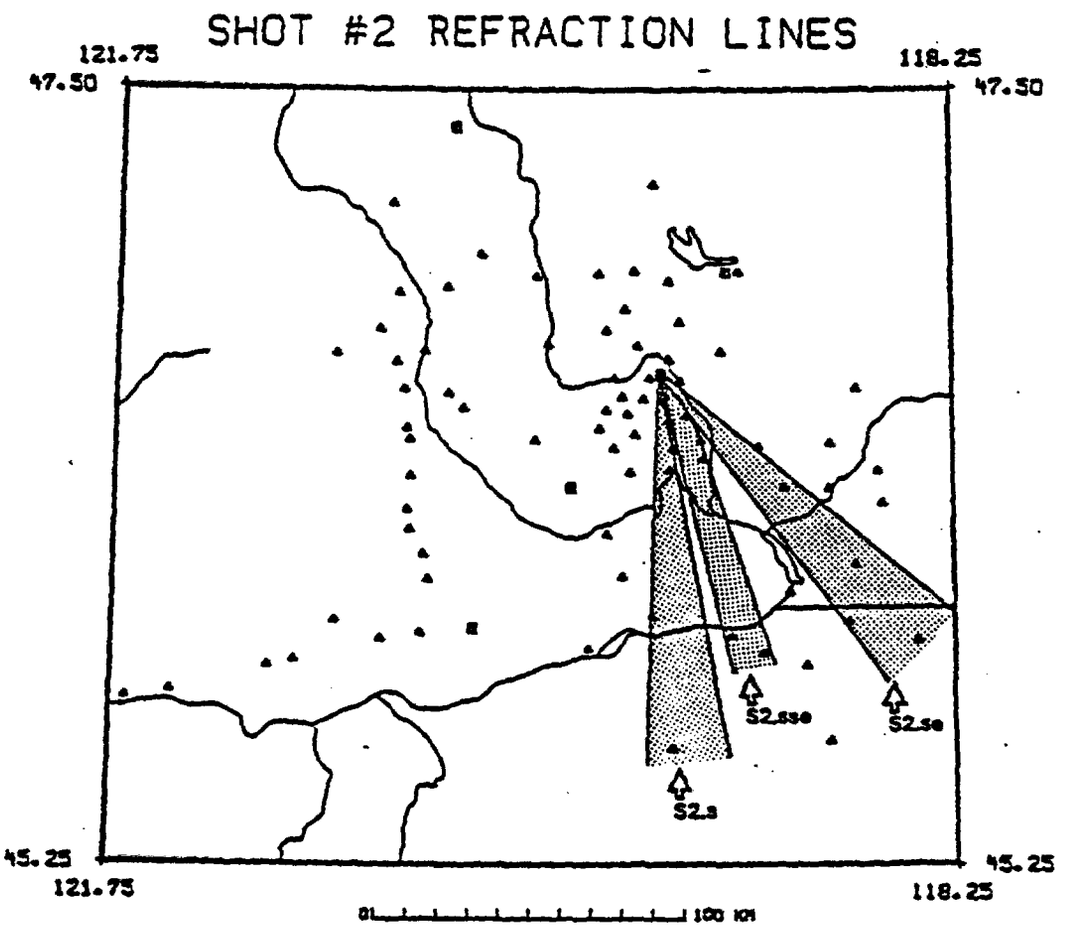

Figure 4.7 Map showing shot #2 refraction lines.

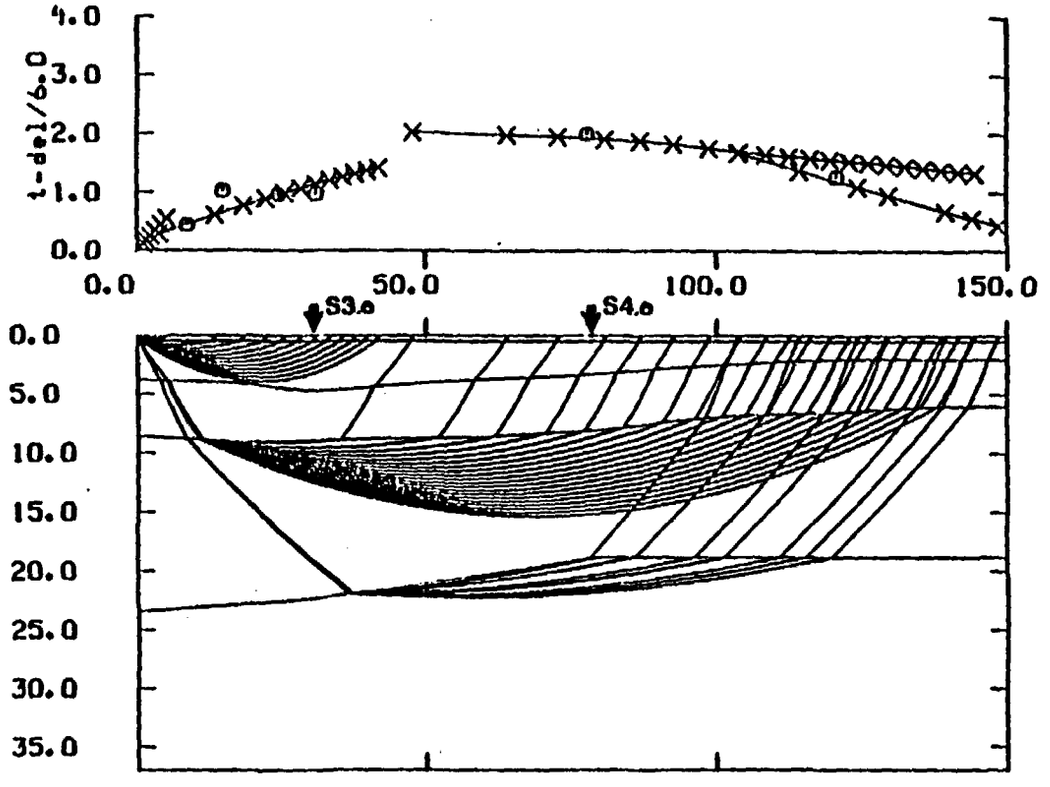

Figure 4.8 Two-dimensional ray-trace model for S2.s. Presentation as in Figure 4.2.

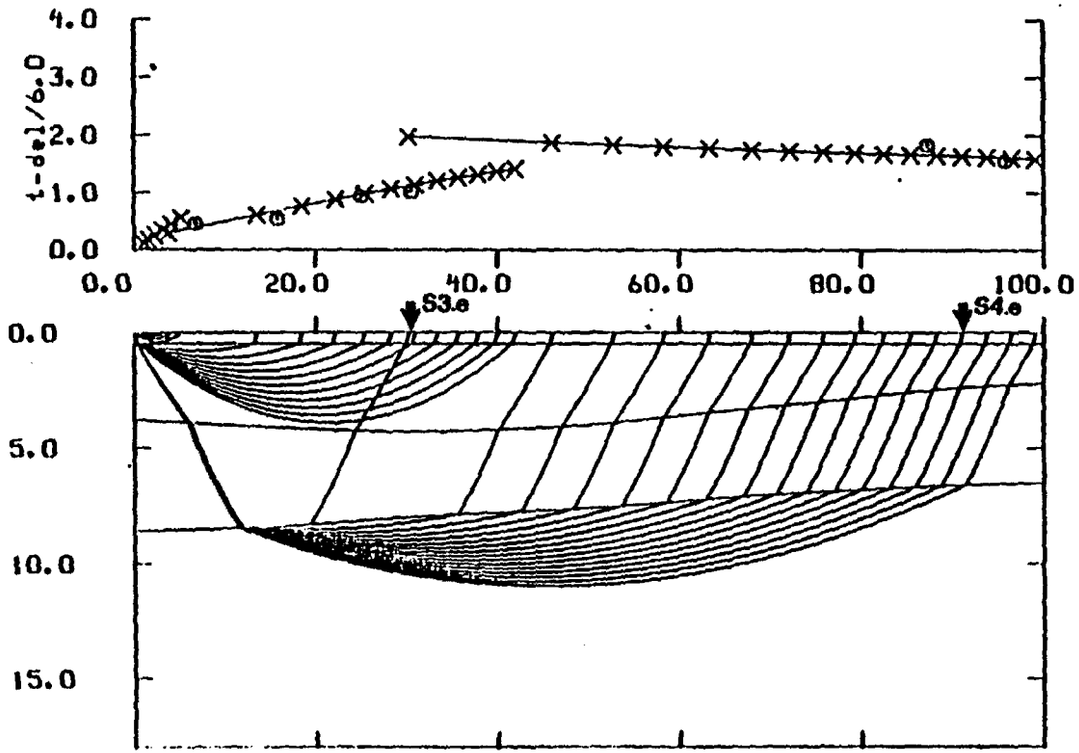

Figure 4.0 Two-dimensional ray-trace model for S2.sse. Presentation as in Figure 4.2.

S2.se

The last and furthest east line stemming from shot #2 is S2.se. The modeled crustal structure along this line is shown in Figure 4.10. Line S2.se crossed S3.e at ETP and S4.e near MFW. ETP is located 39.1km from the source and MFW is 118.6km distant. The deep crustal layer is included in this model because the last arrival time could be from the crystalline basement or the deep crustal layer. The three lines which begin at shot #2 provide good coverage of the southeastern portion of the study area.

Shot #3 Refraction Lines

Three refraction lines that originated from shot #3 are shown on the map in Figure 4.11. These refraction lines are S3.nw, S3.e, and S3.se.

S3.nw

The S3.nw refraction line ran from shot #3, through the permanent network station BRV, passed close to the Shell 1-33 Yakima Minerals Well, and then through NAC another permanent station. A model of the crustal structure along line S3.nw is shown in Figure 4.12. This line began at the USGS line and then intersected two other refraction lines from the experiment – S1.wsw and S4.n. Therefore, with the depth to the bottom of the basalt obtained from the Shell 1-33 Yakima Minerals Well S3.nw has several tie points for each layer in the model. Again, the deep crustal layer is not included in the model because data is lacking beyond 100km.

S3.e

Refraction line S3.e began at shot #3 and then went through the permanent network stations RSW, WTW, and ETP. The crustal structure model for line S3.e is shown in Figure 4.13. This line had tie points from four other refraction lines: the USGS line, the S2.s line, the S2.sse line, and

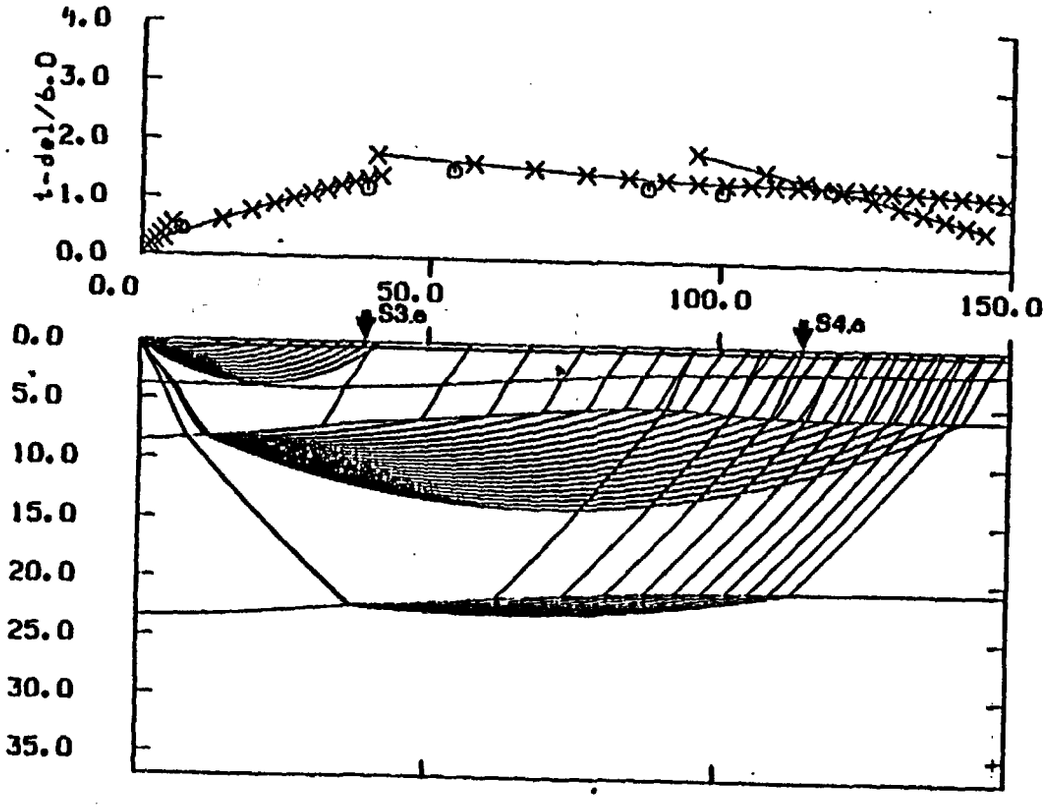

Figure 4.10 Two-dimensional ray-trace model for S2.se. Presentation as in Figure 4.2.

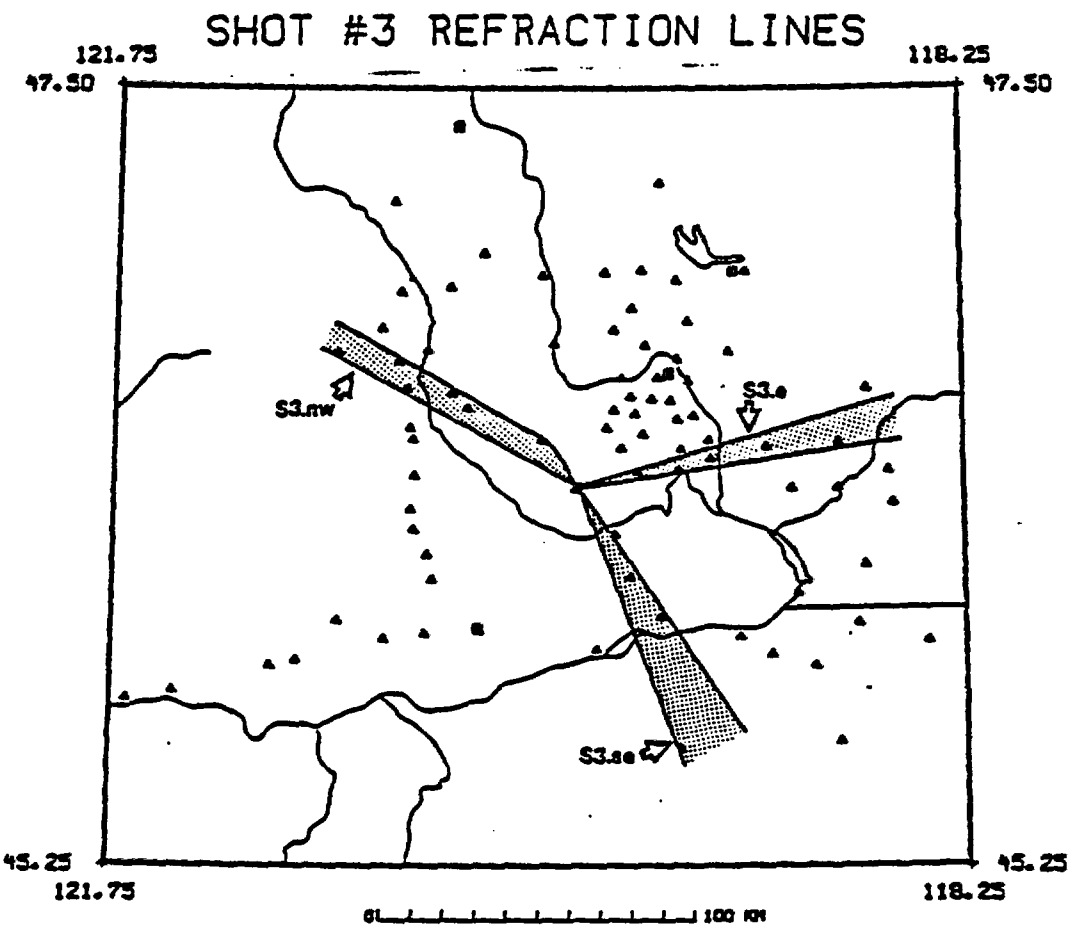

Figure 4.11 Map showing shot #3 refraction lines.

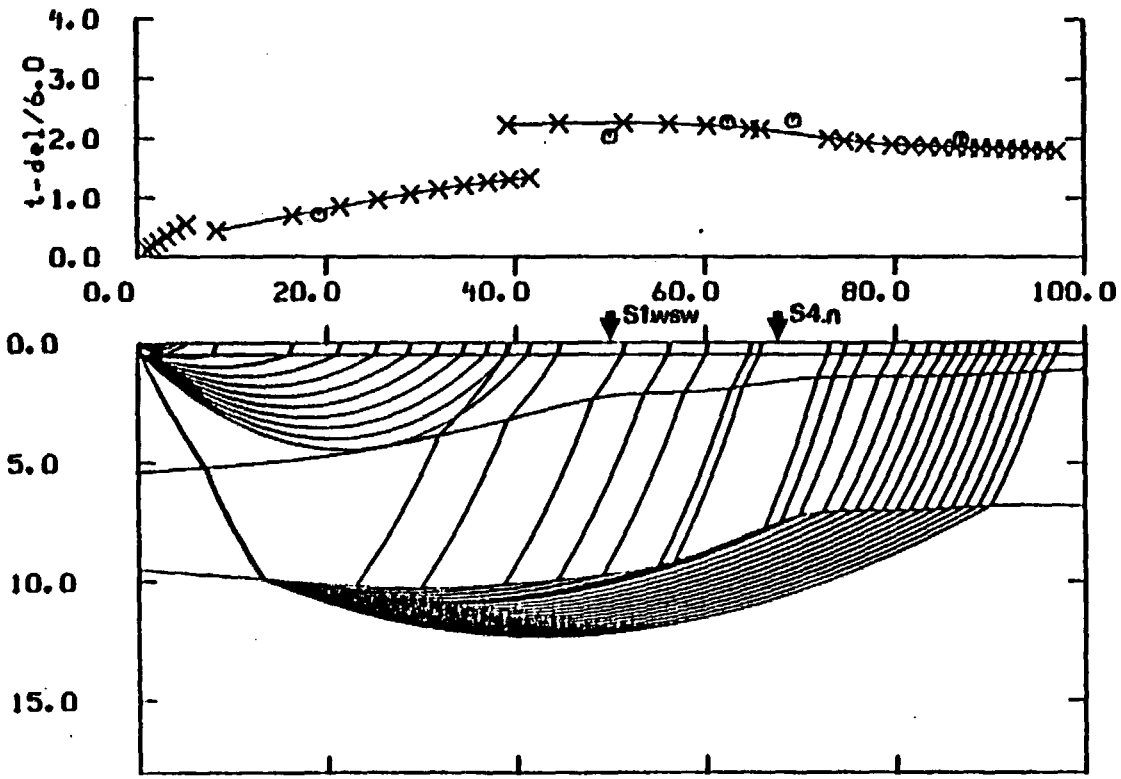

Figure 4.12 Two-dimensional ray-trace model for S3.nw. Presentation as in Figure 4.2.

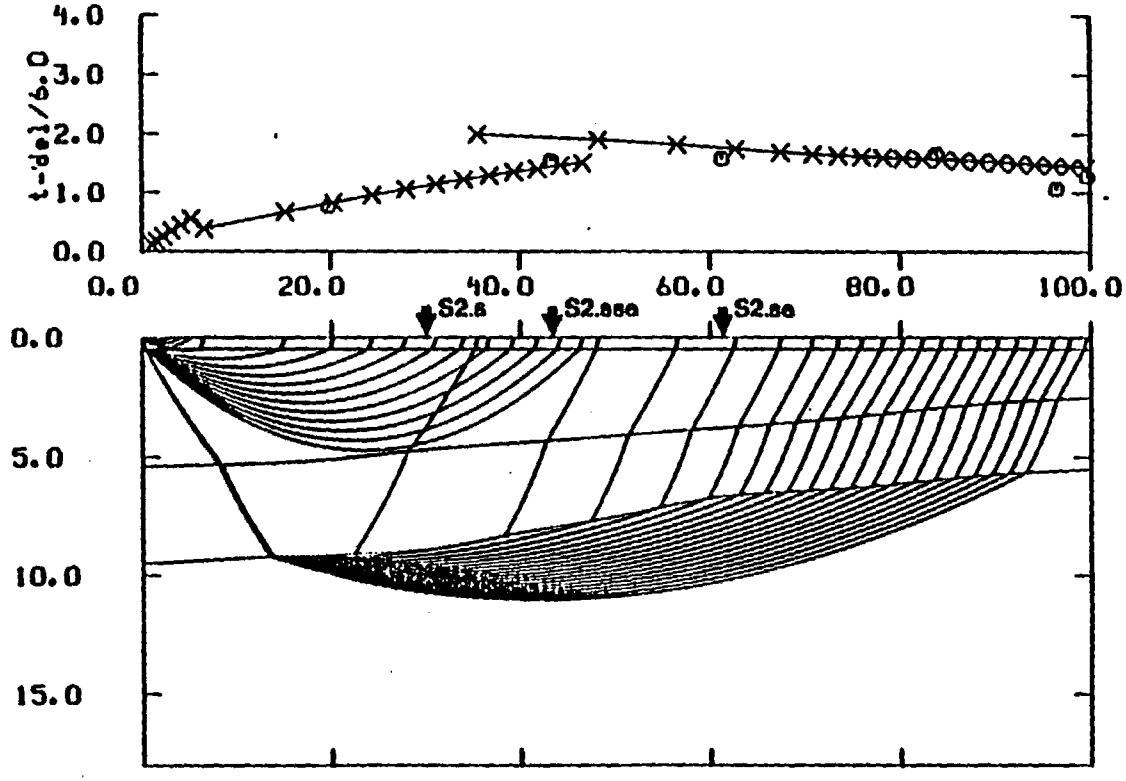

Figure 4.13 Two-dimensional ray-trace model for S3.e. Presentation as in Figure 4.2.

the S2.se line. The early arrival time at a distance of 96.5km on the plot is from station DLY. This station is actually north of the line, but the arrival time has been included on this figure to provide evidence of a shallower crystalline basement to the north.

S3.se

The S3.se refraction line began at shot #3 and headed southeast through the permanent network station PRO. The cross-section along line S3.se is shown in Figure 4.14. The line had tie points from the USGS line at the shot point and from S4.e near PTN (about 49km from the source). Also, the model for the last half of the line is identical to the corresponding segment of the S2.s refraction line.

Shot #4 Refraction Lines

The map in Figure 4.15 shows three refraction lines which originated at shot #4. These lines are S4.n, S4.w, and S4.e.

S4.n

The S4.n refraction line ran north from shot #4 through the permanent network stations YAK, ELL, and TBM. The model for S4.n is shown in Figure 4.16. The northern part of the line was reversed by C.s. Line S4.n had several other tie points: the USGS line at shot #4, line S1.wsw just north of YAK (about 68km from the source), line S3.nw near WNS (about 89km from the source), and line S1.w at ELL (110.5km from the source). Also, the S4.n line passed very close to the Shell 1-33 Yakima Minerals Well located 90.5km from the shot point. This well provided a tie point of 1.5km for the depth to the bottom of the basalt. The basalts are only 0.3km thick in the model at the northern end of the line. The end of the line is near the CRB margin. The slight dip in the basement at a distance of 110km from the source is the

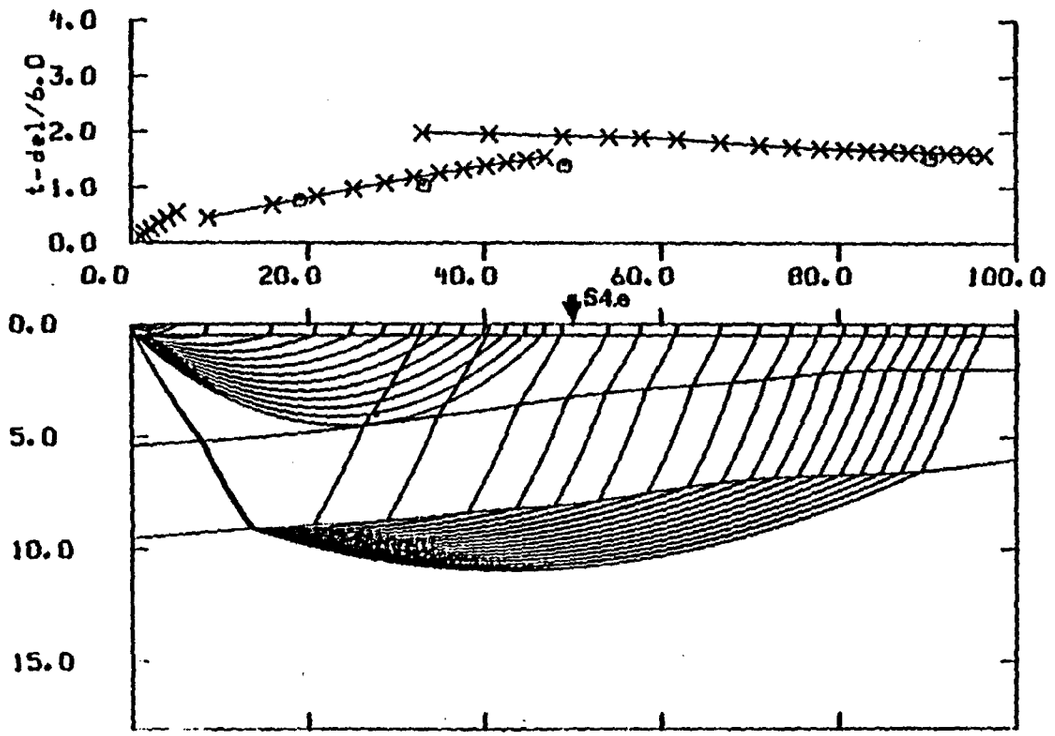

Figure 4.14 Two-dimensional ray-trace model for S3.se. Presentation as in Figure 4.2.

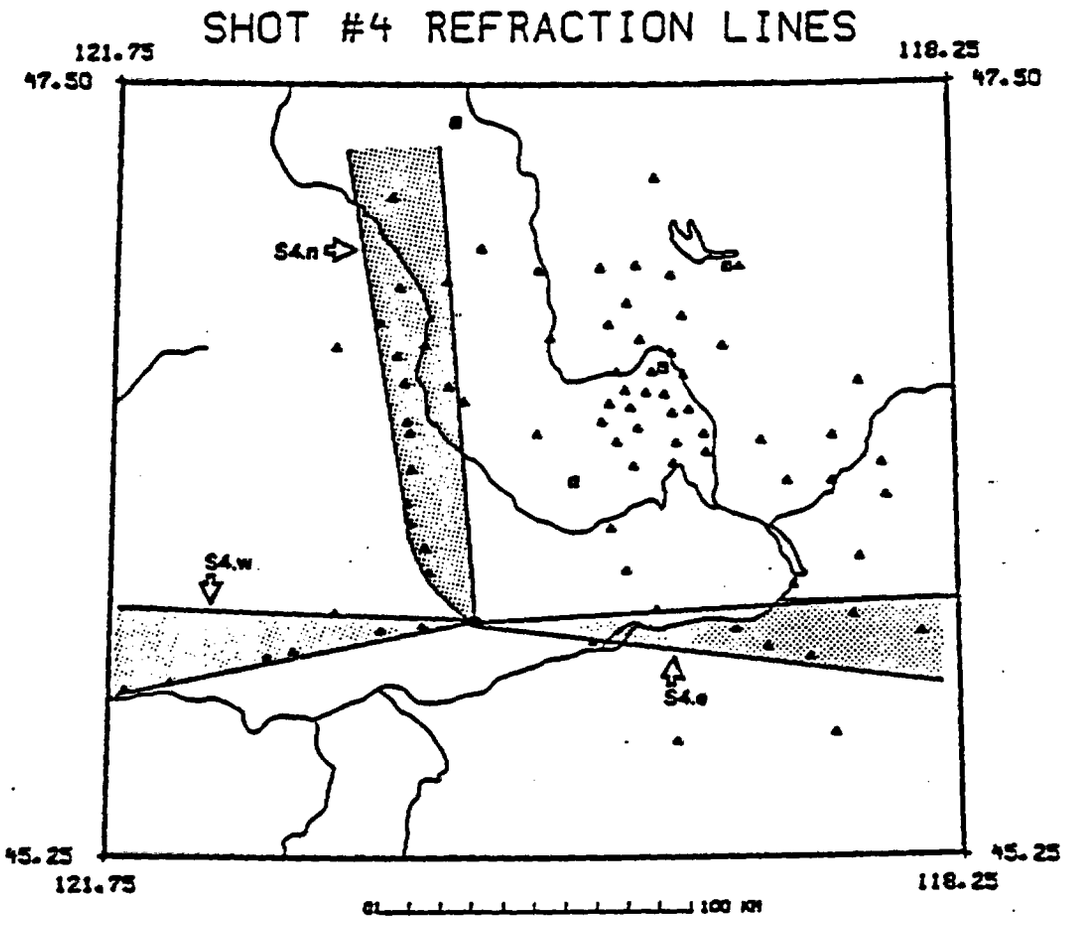

Figure 4.15 Map with shot #4 refraction lines.

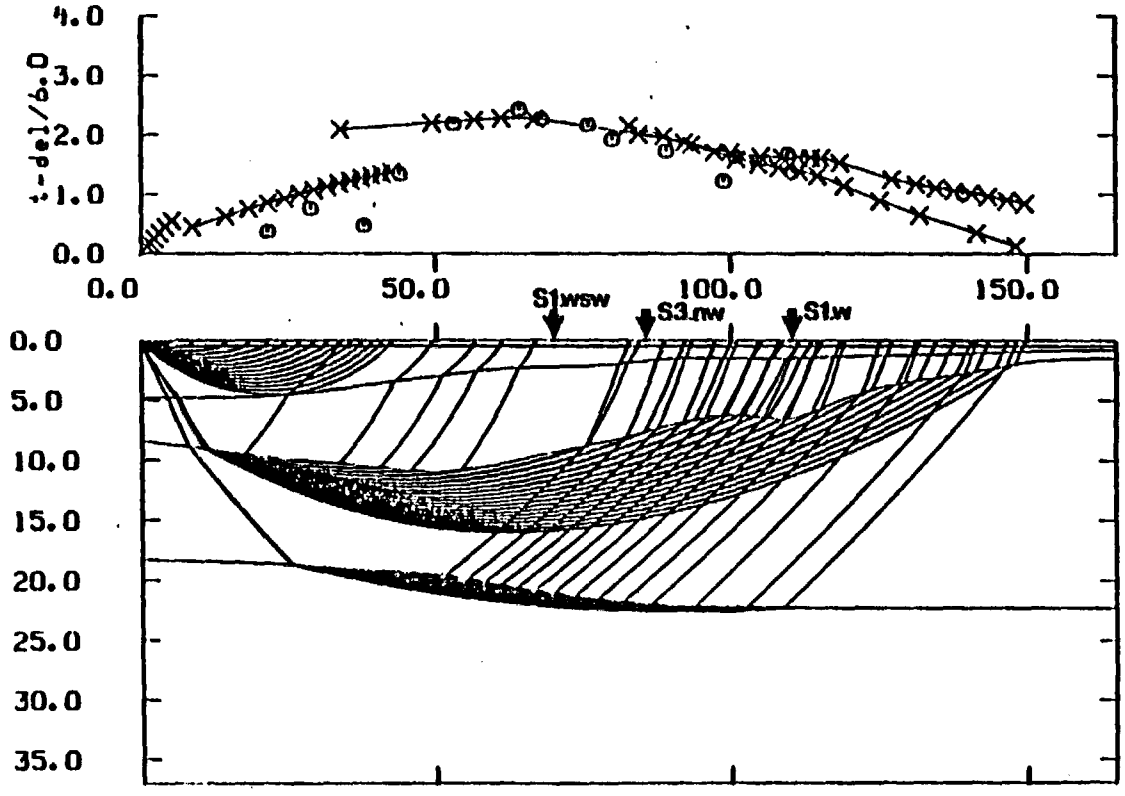

Figure 4.16 Two-dimensional ray-trace model for S4.n. Presentation as in Figure 4.2.

location of the permanent network station ELL and the intersection with line S1.w. The dip in the model at this point was modeled from data along line S1.w. The crystalline basement shallows further north toward the end of the line where it is only 1.5km deep. The deep crustal layer is 18.3km in depth underneath shot #4, then gradually deepens to 22.3km at the northern end of the line.

The first arrival times from stations S05 (21.5km from the source) and S04 (37.9km from the source) were very early. Arrivals from S04 were anomalously early for all four blasts and therefore a systematic error in the recorder is suspected. The arrival time from NAC, which is 98.8km from the source, appears to be early. This station is actually just west of the line but is included to show that the crystalline basement and/or the deep crustal layer shallows to the west. The first arrival time for TBM located at 139.2km from the shot point, appears to be late; however, the noise level before the first arrival is relatively high (refer to Figure 3.2). The amplitude of the first arrival from the deep crustal layer at this distance should be fairly small. Therefore, the real first arrival at TBM could be lost in noise.

S4.w

The S4.w refraction line was designed to run through the permanent network stations GL2 and AUG; however, AUG failed to supply any useful data because of excessive noise. The model for the S4.w line is given in Figure 4.17. This line did not have any other tie points except at the source, therefore the model given here is feasible but hardly unique. Heading west from the shot point, the surface layer thins from 0.5km to 0.3km. This is the only line that has been modeled without a constant 0.5km-thick surface layer. The S4.w refraction line ends about 50km north of the southwest corner of the map shown in Figure 4.15. This location is also near the

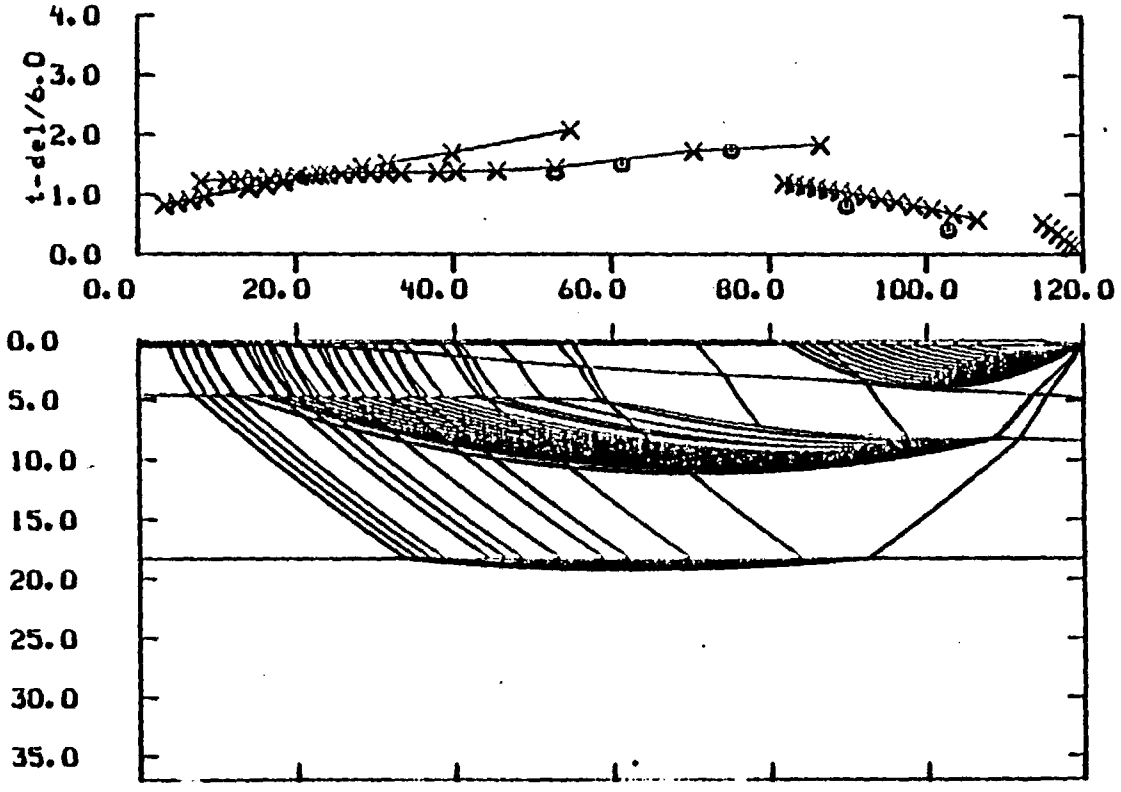

Figure 4.17 Two-dimensional ray-trace model for S4.w. Presentation as in Figure 4.2.

Columbia River Basalt Group margin. Therefore the basalts, the second layer of the model, thin to the west until they are only 0.2km thick. The deep crustal layer along this line has been modeled as a flat layer 18.3km deep. The depth seems to be an upper bound for the actual deep crustal layer because 99km from the source the arrival time for this layer and the crystalline basement are nearly the same. This distance is the location of the furthest west station (SW8) along the line. If the deep crustal layer were to shallow going west, the arrival time for a refraction from this layer would be earlier than the first arrival time at SW8. Therefore, the deep crustal layer is probably not shallower than 18.3km.

S4.e

The S4.e refraction line ran through the permanent network stations PAT and MFW. A model for the crustal structure along S4.e is shown in Figure 4.18. This line intersected several other refraction lines besides the USGS line at the source. Near PTN (about 58km from the source), the S4.e line crossed both S2.s and S3.se. S4.e intersected S2.sse between HAT and CSP (83.5km and 94.0km from the source, respectively). Also, near MFW (about 143km from the source), the S4.e line crossed S2.se. Three arrivals beyond 100km helped to constrain the depth to the deep crustal layer. Underneath the shot point the depth is 18.3km increasing to 20.8km at the end of the line.

Cannon Mine Refraction Lines

Two refraction lines have been analyzed using Cannon Mine blasts as sources (Figure 4.19). These lines, C.s and C.sse, were interpreted to confirm that the crystalline basement is substantially shallower in the northernmost part of the study area and also to reverse the S4.n line.

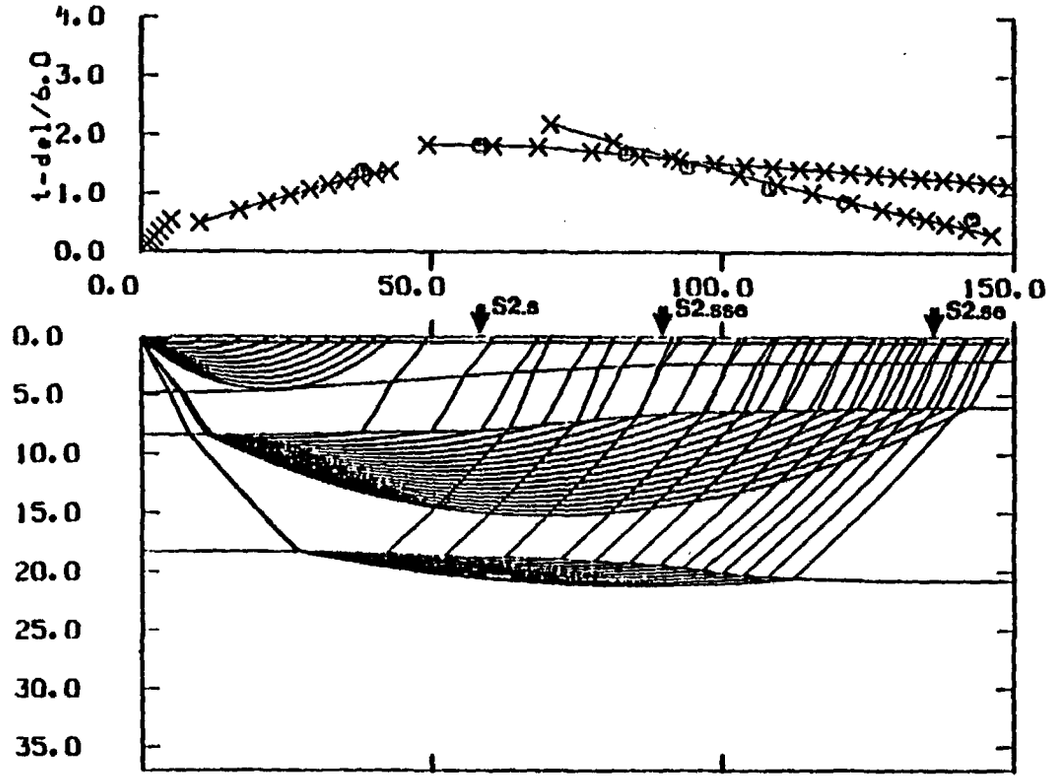

Figure 4.18 Two-dimensional ray-trace model for S4.e. Presentation as in Figure 4.2.

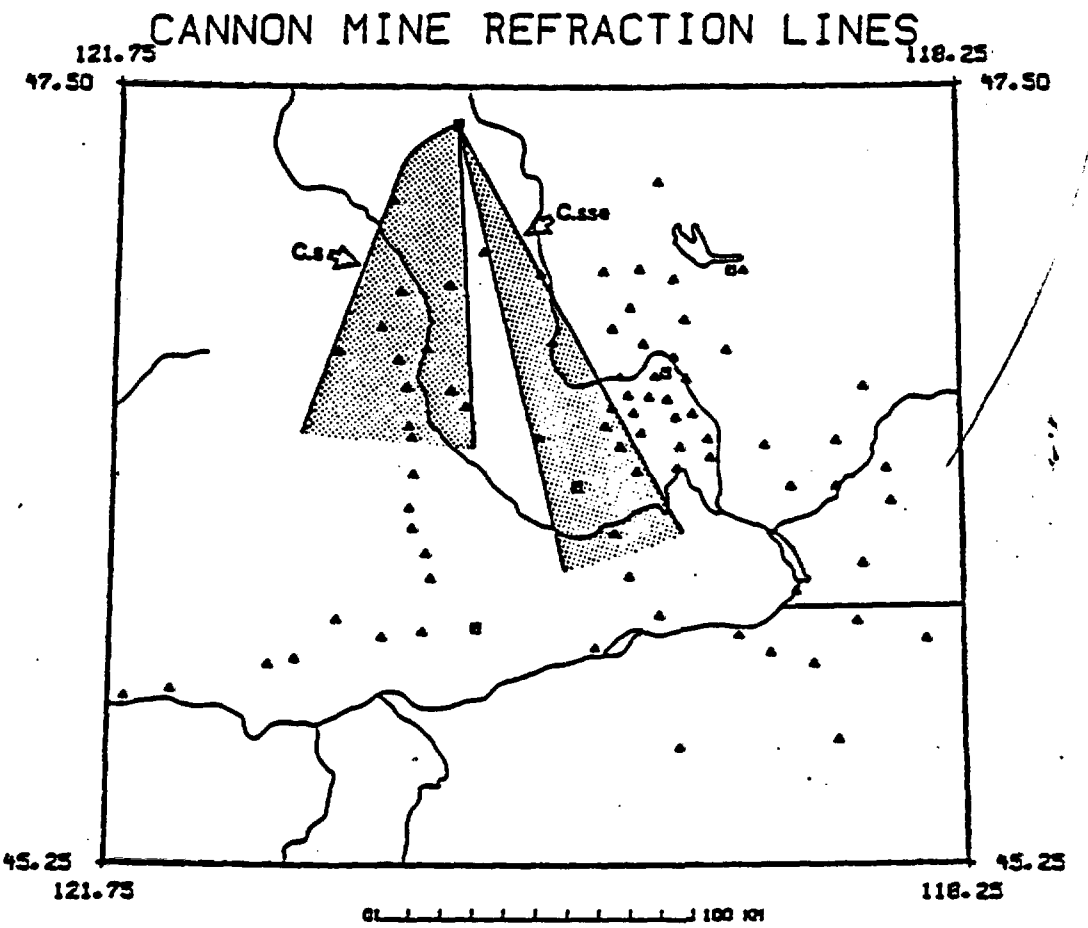

Figure 4.19 Map showing Cannon Mine refraction lines.

C.s

Refraction line C.s is the reversal of the northern half of line S4.n. The model, identical to the one derived for S4.n, is shown in Figure 4.20. Line C.s, originating at the Cannon Mine, crossed S1.w at ELL (56.0km from the source), and continued as far south as YAK (97.5km from the source). The results clearly show that the crystalline basement is very shallow near the source (1.5km) and then deepens heading south.

C.sse

The refraction line C.sse originated at the Cannon Mine and then ran south-southeast through the center of the study area. The model displaying the crustal structure along this line is shown in Figure 4.21. Even though there are only four data points along this line, the model has been constrained by three other refraction lines. C.sse crossed S1.w at VTG (54.7km from the source), intersected S1.wsw about 75km from the source, and crossed the USGS line near the third shot point. Also, just northwest of VTG, the Shell 1-29 Bissa Well is relatively close to this line.

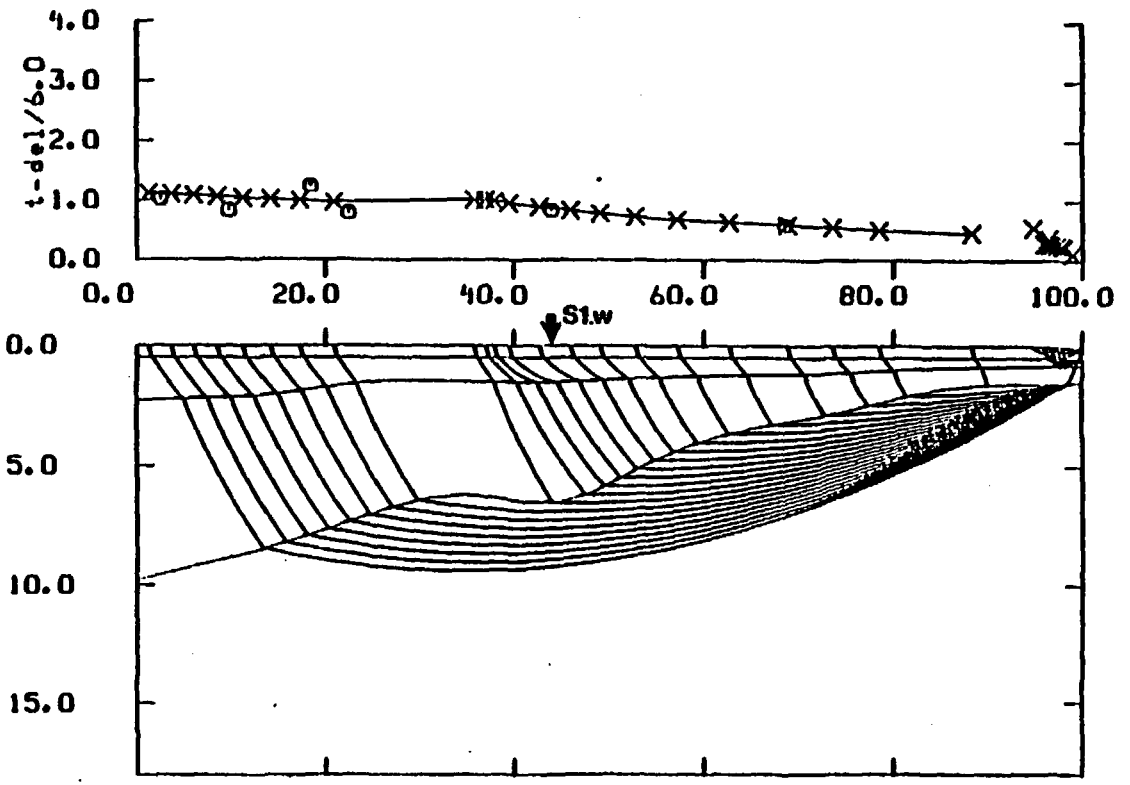

Figure 4.20 Two-dimensional ray-trace model for C.s. Presentation as in Figure 4.2.

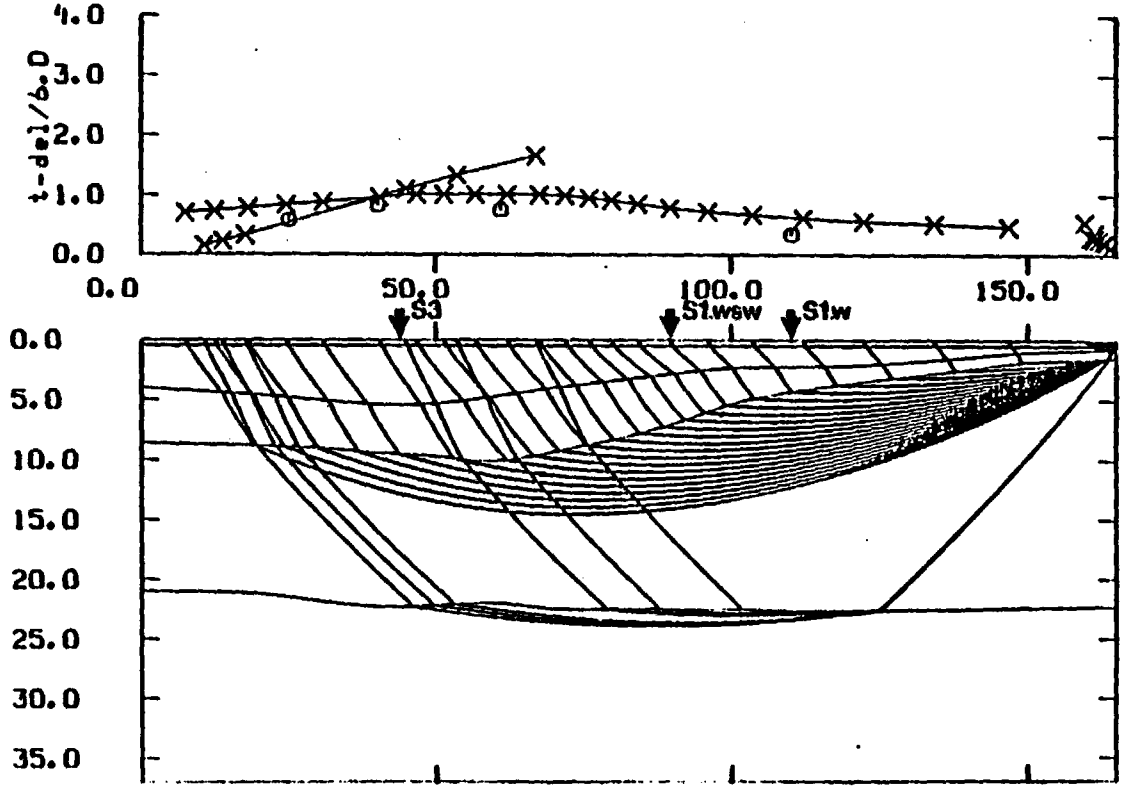

Figure 4.21 Two-dimensional ray-trace model for C.sse. Presentation as in Figure 4.2.

Chapter V -- DISCUSSION

The results of modeling the refraction data have led to the creation of a three-dimensional model for most of the study area. The original goals to determine the depth to the bottom of the basalt, to verify the existence of low-velocity sediments beneath the basalt, to determine the depth to the crystalline basement, and to use the interpretation of the USGS refraction line as a guide in evaluating the other refraction lines in the area were accomplished. My results along the USGS line are in close agreement with the results obtained by Catchings and Mooney (1985).

The information obtained from the deep boreholes in the northern part of the study area proved invaluable in developing the basalt layer of the model. A contour map showing the depth to the bottom of the basalts is given in Figure 5.1. The basalt margin has been included on this map for reference. Recall that in my model a 0.5km-thick surface layer lies on top of the basalts. The contour map was created by plotting depths from each refraction line. Contours were then interpolated between these values. The thickest area of basalts is inside the 5km contour near shot #3 where the basalts extend to a depth of 5.4km.

The basalts of the CRB are not as thick as earlier estimates indicated. Cantwell et al. (1965), in a deep resistivity study of the Pacific Northwest, identified the upper 10km to 15km as the CRB. The analysis of a gravity study conducted by Konicek (1974) agreed with the results determined by Cantwell. Rohay and Malone (1983) and Malone et al. (1983) analyzed blast data from eastern Washington, creating a two-layered model by using a time

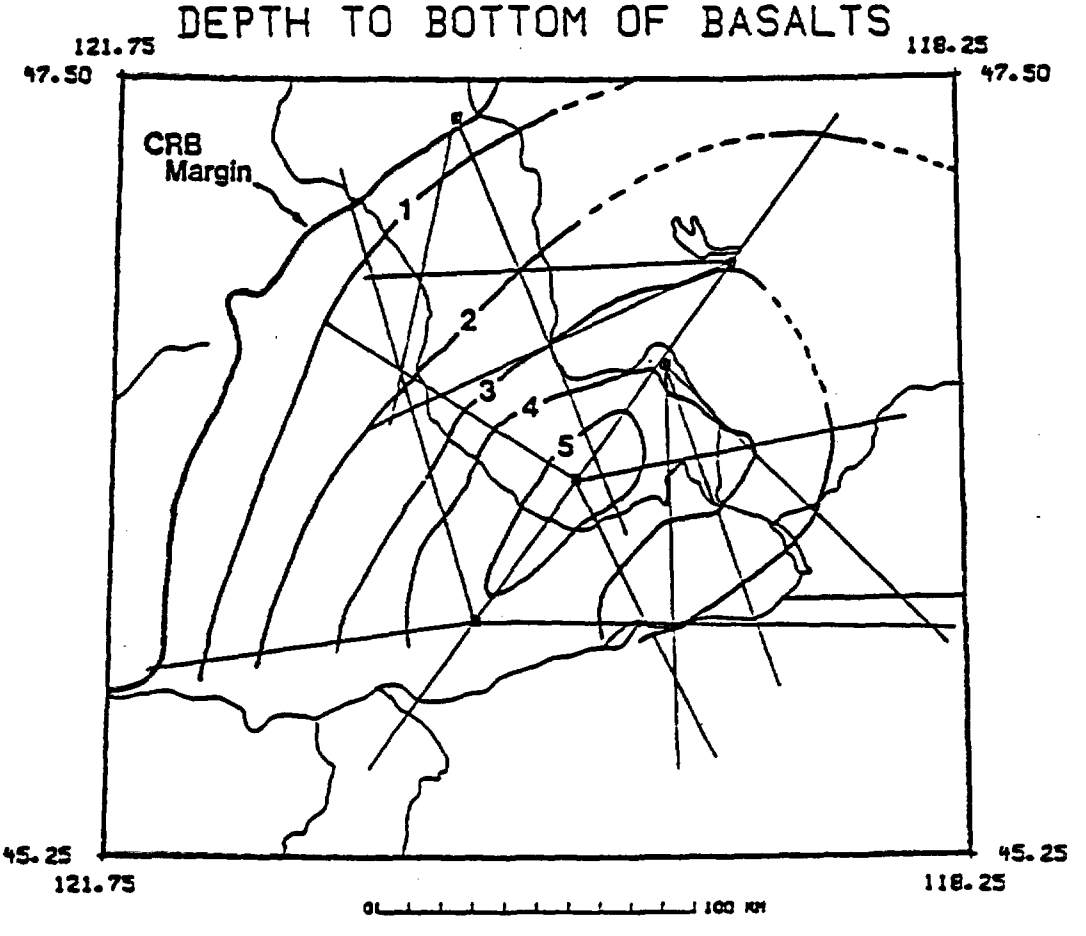

Figure 5.1 Contour map showing depth to bottom of basalt and refraction lines. Contours are in kilometers. The 0.5km surface layer is included in the calculation of this depth.

term technique. The top layer is analogous to my first three layers and the second layer is the crystalline basement. These authors state that the top layer could be composed of up to 10km of basalt; however, they also suggest that a layer of low-velocity, low-density sediments may exist between the basalts and the crystalline basement.

The existence of a low-velocity sedimentary layer agrees nicely with my results. Figure 5.2 shows an isopach map of the low-velocity sediments between the basalts and the crystalline basement. This map was created by subtracting the values on the previous figure from the values on the next figure. The existence of the sedimentary layer beneath the basalts is consistent with the hypotheses presented by Gresens et al. (1981) and Campbell (in preparation (b)). Stanley (1984) also modeled a sedimentary layer beneath the basalts with the basalts extending to a maximum depth of 3.5km. He analyzed two magnetotelluric profiles recorded in the state of Washington. Furthermore, Cowan and Potter (in press) have included a layer of sediments beneath the basalts. They have modeled approximately 7km of basalts and 1km to 2km of sediments beneath the basalts near the center of the basin.

Figure 5.3 shows a contour map of the depth to the top of the crystalline basement. Rohay and Malone (1983) and Malone et al. (1983) determined a depth to the crystalline basement ranging from 3km to approximately 11km. Their results for the depth to the crystalline basement are greater in most of the study area than the depths that I have determined. This discrepency is probably due to the inclusion of the low-velocity zone in my model, which raises the actual depth of the basement rock.

The crystalline basement shallows in the north to 1.5km near the Cannon Mine. This shallowing is reasonable since exposures of gneiss have been

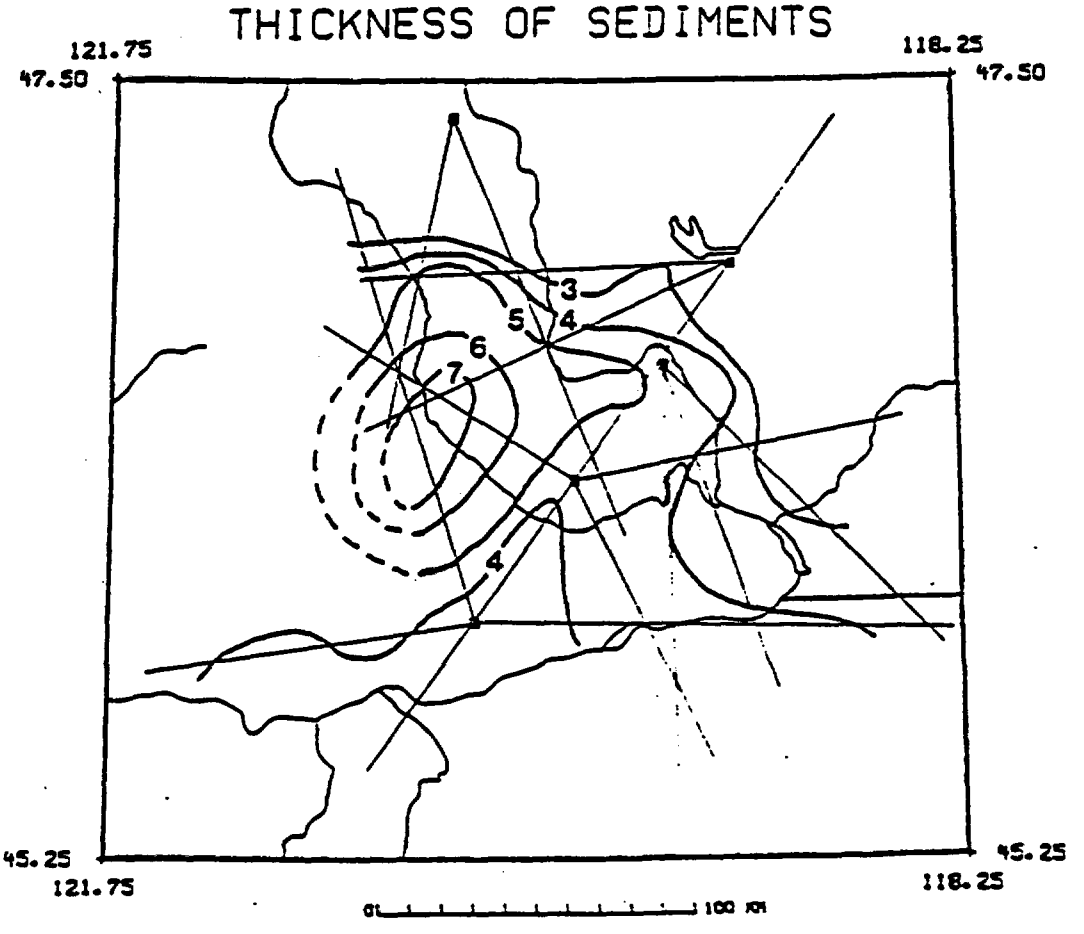

Figure 5.2 Isopach contour map showing thickness of Tertiary sediments between basalts and basement. Refraction lines are also present. Contours are in kilometers.

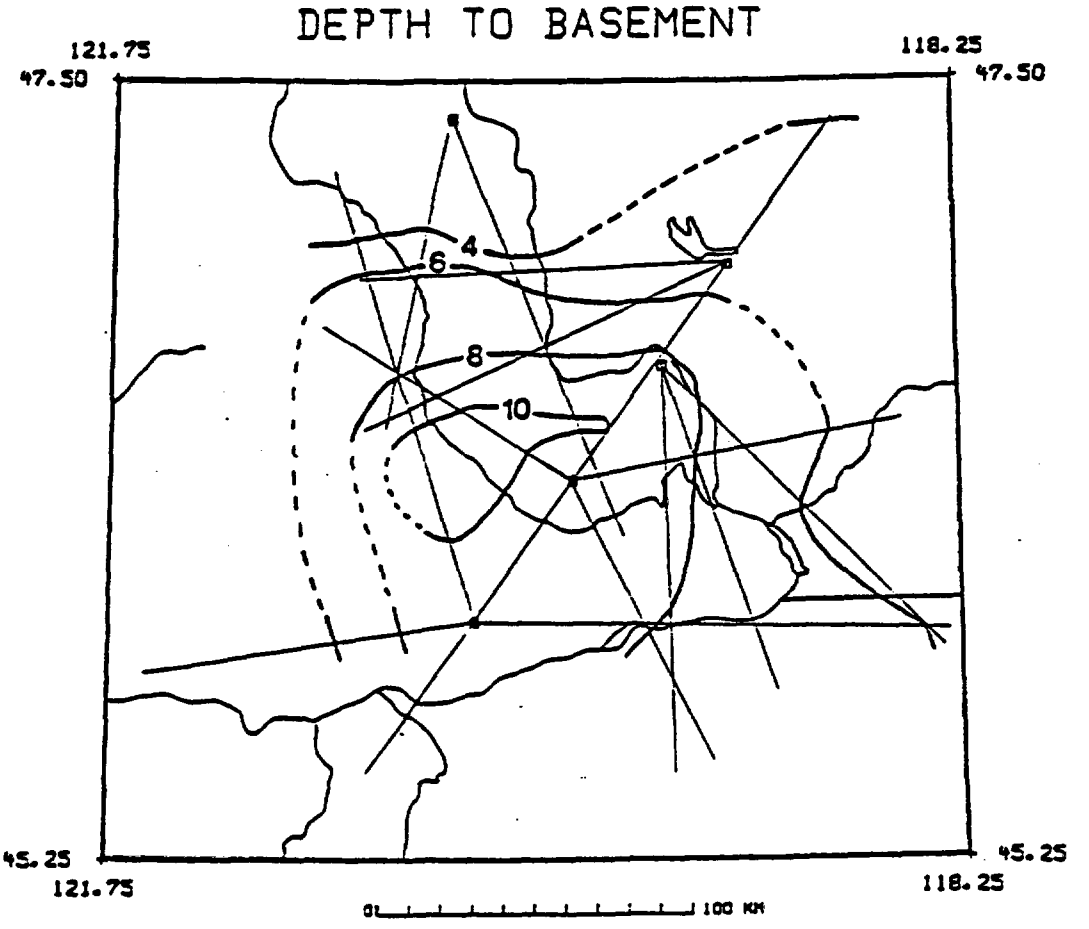

Figure 5.3 Contour map showing depth to top of crystalline basement and refraction lines. Contours are in kilometers.

found in the area (Gresens et al., 1981). In addition, Silling (1979) determined from gravity data that the depth to the basement rock in the Chiwaukum Graben, just north of the study area, is probably about 2km.

The deep crustal layer has been defined mainly from data along the USGS line, S4.n, and S4.e. This layer is shallower in the southern part of the study area where it is about 18km. The deep crustal layer gradually deepens in the north to a maximum depth of 23.5km near shot #2. The existence of this layer could explain some of the results determined by Hill (1972). Hill analyzed data from a 600km-long unreversed seismic refraction survey that extended due south from the Canadian border across the Columbia Plateau into eastern Oregon. He concluded that the depth to the Moho shallows to approximately 20km through the central basin. He may have actually been seeing arrivals from this deep crustal layer (7.2km/s), which would have a faster apparent velocity up dip going north to south.

A discussion of the results is not complete without mentioning the possible errors involved in the analysis. In addition to the error due to topography cited earlier, other errors include the difference between picked and predicted arrival times, the imprecision of the velocity model, the approximation of stations along a straight line, and the modeling of only one or two arrivals along some of the refractors. Performing a rigorous quantitative error analysis on refraction data proves to be a very difficult task – especially when a low-velocity layer is included in the model. However, the standard deviation between observed and modeled arrival times (σ_t) can be calculated. A complete list of these errors is included in Appendix II.

Errors for the velocity of each layer can be estimated. These estimated errors are the following: $\sigma_{v_1} = 1.30$km/s, $\sigma_{v_2} = 0.20$km/s, $\sigma_{v_3} = 0.50$km/s, $\sigma_{v_4} = 0.30$km/s, and $\sigma_{v_5} = 0.40$km/s. The error in the first layer is large

because of the surface layer approximation (the basalts are at the surface in some areas). Having determined the traveltime error and the velocity error, a resolution length (σ_z) can be calculated for the three refractors. These errors are listed in Table V.1.

TABLE V.1 Resolution of each Refractor

Refractor	σ_t (s)	σ_v (km/s)	σ_z (km)
basalt	0.19	0.28	0.03 *
basement	0.14	0.20	0.30
deep crustal	0.10	0.20	0.66

* The error due to topography (surface layer approximation) is actually the dominant error for this refractor.

The boundary for the crystalline basement is very well determined. This resolution length, calculated for a depth of 8.0km. is an average for the refractor. The resolution length for the deep crustal refractor was calculated for a depth of 20.5km. The resolution for both of these refractors, as expected, becomes worse with depth.

The most difficult boundary to determine is the interface between the basalts and the low-velocity sediments. The deep boreholes in the northern part of the study area provide fixed points for the depth to this interface and absolute proof of the existence of the low-velocity layer in some areas. Also, the data from the USGS record sections exhibit shadow zones from a low-velocity layer (Catchings and Mooney, 1985). The shadow zones are not evident on the record sections from the other refraction lines because of the sparse station spacing, however a delay in the arrivals from the crystalline basement can be seen. Since no rays bottom in the low-velocity layer. the boundary was set by observing the delayed first arrivals from the crystalline basement, cross-over distances between the basalts and the basement, and

depths from the deep boreholes.

Figure 5.4 shows traveltime curves for three different models of lines S1.w and S4.n. The first traveltime curve is from my original model with a low-velocity layer. The second traveltime curve is from a model with the low-velocity layer half as thick and the last traveltime curve is from a model without the low-velocity layer. The depth to the crystalline basement had to be altered slightly for the models to compensate for the adjustments and removal of the low-velocity layer.

On the traveltime curves for the original model the refracted arrivals from the basalts are plotted as ending at approximately 26km on S1.w and 43km on S4.n. Refracted waves actually continue to arrive. However, because of the presence of the low-velocity layer the amplitudes of the arrivals have been greatly attenuated at these distances. The first arrivals from the crystalline basement appear to be late on the traveltime curves with only half of the low-velocity layer and without the low-velocity layer. With such a small low-velocity layer and without this layer, the first arrivals from the basalt refractor do not attenuate as rapidly. These models provide evidence that the low-velocity layer exists and the boundary between the sediments and the basalts has been modeled relatively accurately. By observing the traveltime curves for S1.w and S4.n. a crude error approximation for the thickness of the low-velocity layer can be set at 25%.

In conclusion, through the analysis of deep borehole data and seismic refraction data, a geologically feasible three-dimensional crustal model of the Columbia Basin has been created.

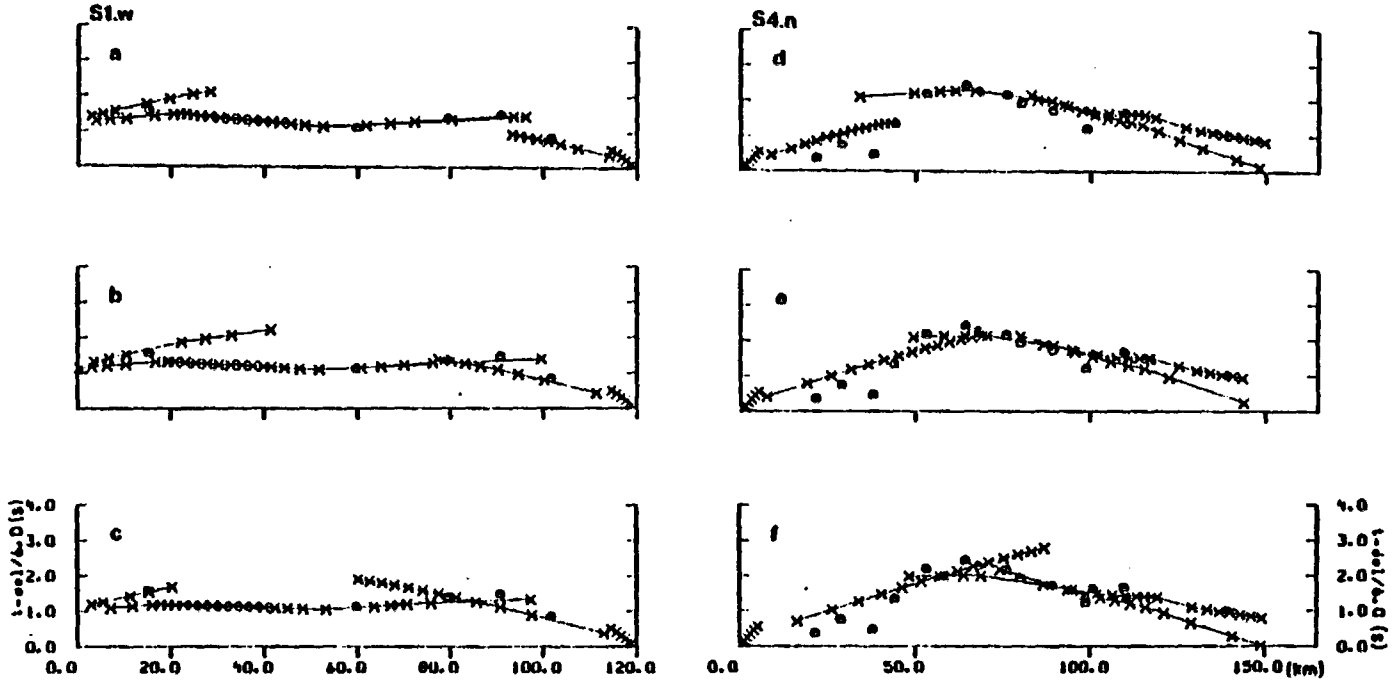

Figure 5.4 Reduced traveltime curves for three different models along S1.w (a,b,c) and S4.n (d,e,f): (a) and (d) are for the original models with a low-velocity layer, (b) and (e) are for a model with a low-velocity layer half as thick, and (c) and (f) are for a model without a low-velocity layer. The observed data are shown as open circles and the calculated data, obtained by ray-tracing, are shown as x's.

BIBLIOGRAPHY

Campbell, N.P., Stratigraphy and Hydrocarbon Potential of the Northwestern Columbia Basin Based on Recent Drilling Activities, *Rep. SD-BWI-TI-265, Rockwell Hanford Operations,* Richland, Washington, in preparation (a).

Campbell, N.P., Structural Geology along the Columbia River Basalt Margin, Wenatchee Area, Washington, *Rep. RHO-BWI-SA-325, Rockwell Hanford Operations,* Richland, Washington, in preparation (b).

Cantwell, T., Nelson, P., Webb. J., and Orange, A.S., Deep Resistivity Measurements in the Pacific Northwest, *Journal of Geophysical Research, 70,* 1931-1937, 1965.

Catchings, R.D. and Mooney, W.D., Crustal Structure of the Columbia Plateau, Abstract in *Earthquake Notes, 55,* No. 1, p. 22, Eastern Section of the Seismological Society of America, 1985.

Cerveny, V., Molotkov, I.A., and Psencik, I., *Ray Method in Seismology,* Univerzita Karlova, Praha, 1977.

Cowan, D.S. and Potter, C.J., Continent-Ocean Transect B3: Juan de Fuca Spreading Ridge to Montana Thrust Belt, *Geological Society of America Continent-Ocean Transect Series,* in press.

Dobrin, M.B., *Introduction to Geophysical Prospecting,* 3rd ed., McGraw-Hill, Inc., New York, 1976.

Goff, F.E. and Myer, C.W., Structural evolution of east Umtanum and Yakima Ridges, south-central Washington, *Geological Society of America Abstracts with Programs, 10,* No. 7, p. 408, 1978.

Gresens, R.L., Geology of the Wenatchee and Monitor quadrangles, Chelan and Douglas counties, Washington, *Bulletin Washington State Geology and Earth Resources Division, 75,* 1983.

Gresens, R.L. and Stewart, R.J., What lies beneath the Columbia Plateau?, *Oil & Gas Journal,* 157-164, August 3, 1981.

Gresens, R.L., Naeser, C.W., and Whetten, J.T., Stratigraphy and age of the Chumstick and Wenatchee Formations: Tertiary fluvial and lacustrine rocks, Chiwaukum graben, Washington: Summary, *Geological Society of America Bulletin, Part I, 92,* 233-236; *Part II, 92,* 841-876, 1981.

Healy, J.H., Mooney, W.D., Blank, H.R., Gettings, M.E., Kohler, W.M., Lamson, R.J., and Leone, L.E., Saudi Arabian seismic deep-refraction profile: final project report, *U.S. Geological Survey Saudi Arabian Mission Report 02-37,* Jiddah, Saudi Arabia, 1982.

Hill, D.P., Crustal and Upper Mantle Structure of the Columbia Plateau from Long Range Seismic-Refraction Measurements, *Geological Society of America Bulletin, 83,* 1639-1648, 1972.

Konicek, D.L., Geophysical Survey in South-Central Washington, *Master's Thesis,* University of Puget Sound, Tacoma, Washington, 1974.

Laval, W.N., Stratigraphy and structural geology of portions of south-central Washington, *Ph.D. Thesis,* University of Washington, Seattle, Washington, 1956.

Lewis, D.S., Mystery of the Columbia Plateau, *Oil and Gas Investor, 2,* 29-33, 1982.

Malone, S.D. et al., Annual Technical Report 1983 on Earthquake Monitoring of Eastern and Southern Washington, *Geophysics Program,* University of Washington, Seattle, Washington, 1983.

McKee, B., *Cascadia: The Geologic Evolution of the Pacific Northwest,* McGraw-Hill, Inc., New York, 1972.

Myers, C.W. and Price, S.M. et al., Geologic Studies of the Columbia Plateau: A Status Report, *Rep. RHO-BWI-ST-4, Rockwell Hanford Operations*, Richland, Washington, 1979.

Rohay, A.C. and Malone, S.D., Crustal Structure of the Columbia Plateau Region, Washington, *Rep. RHO-BW-SA-289P, Rockwell Hanford Operations*, Richland, Washington, 1983.

Rohay, A.C., personal communication, 1985.

Russell, I.C., A geological reconnaissance in central Washington, *U.S. Geological Survey Bulletin*, No. 108, 1893.

Shirley, K., Columbia Plateau Activity Booms: Magnetotellurics Offers New Looks, *American Association of Petroleum Geologists Explorer*, November, 1984.

Silling, R.M., A Gravity Study of the Chiwaukum Graben, Washington, *Master's Thesis*. University of Washington, Seattle, Washington, 1979.

Smith, G.O., Anticlinal mountain ridges in central Washington, *Journal of Geology, 11*, 166-177, 1903.

Stanley, W.D., Tectonic Study of Cascade Range and Columbia Plateau in Washington State Based Upon Magnetotelluric Soundings, *Journal of Geophysical Research, 89*, 4447-4460, 1984.

Swanson, D.A., Wright, T.L., and Helz, R.T., Linear vent systems and estimated rates of magma production and eruption for the Yakima basalt on the Columbia Plateau, *American Journal of Science, 275*, 877-905, 1975.

Tabor, R.W., Frizzell, V.A., Jr., Vance, J.A., and Naeser, C.W., Ages and stratigraphy of lower and middle Tertiary sedimentary and volcanic rocks of the central Cascades, Washington: Application to the tectonic history of the Straight Creek fault, *Geological Society of America Bulletin, 95*, 26-44, 1984.

Waters, A.C., Geomorphology of south-central Washington, illustrated by the Yakima East quadrangle, *Geological Society of America Bulletin, 66,* 663-684, 1955.

APPENDIX I

The distance from the shot point and the arrival time for each station along a refraction line are listed in the following table. Data from the USGS line are not included.

TABLE AI.1 Data from Refraction Lines

Refraction Line	Station	Distance (km)	Time (s)
S1.w	RC1	18.33	3.92
	NE1	29.09	6.33
	NE2	40.53	8.15
	VTG	60.26	11.17
	ELL	104.73	19.04
S1.wsw	RC1	18.33	3.92
	SYR	34.30	6.86
	NE4	61.16	11.78
	KIT	96.83	17.61
	SLH	109.39	19.74
	YAK	113.50	20.37
S2.s	GBL	8.74	1.90
	SAN	14.90	3.51
	PLR	24.53	5.05
	HOR	31.00	6.13
	PTN	77.93	14.99
	BUT	120.73	21.39
S2.sse	WHI	6.82	1.59
	MJ2	15.83	3.18
	WNP	25.10	5.13
	WIW	30.60	6.12
	HAT	87.36	16.39
	CSP	95.85	17.53
S2.se	WHI	6.82	1.59
	ETP	39.07	7.69
	PSC	53.85	10.49
	JON	87.29	15.82
	WRM	100.04	17.89
	MFW	118.58	21.06

S3.nw	BRV	19.28	3.94
	KIT	50.02	10.37
	SLH	62.51	12.69
	WNS	69.40	13.87
	NAC	87.09	16.51
S3.e	RSW	19.80	4.06
	WIW	43.38	8.78
	ETP	61.32	11.80
	SRR	83.90	15.65
	DLY	96.47	17.15
	GRN	99.72	17.90
S3.se	PRO	19.09	3.95
	RYD	33.26	6.58
	PTN	49.11	9.58
	BUT	90.40	16.58
S4.n	S05	21.53	3.97
	S06	28.77	5.56
	S04	37.86	6.79
	S03	43.97	8.67
	S02	53.14	11.05
	S01	64.36	13.16
	YAK	68.09	13.62
	KIT	76.00	14.84
	SLH	80.11	15.28
	WNS	89.19	16.59
	NAC	98.85	17.70
	N03	100.90	18.44
	N02	109.78	19.97
	ELL	110.50	19.79
	TBM	139.25	24.22
S4.w	SW1	17.06	3.25
	SW2	30.09	5.82
	GL2	44.62	9.18
	SW3	58.51	11.26
	SW6	67.04	12.55
	SW8	98.99	17.82
S4.e	PAT	38.24	7.76
	PTN	58.24	11.53
	HAT	83.53	15.60
	CSP	94.02	17.13
	MFC	108.09	19.11
	WRM	121.01	21.04
	MFW	142.84	24.39

C.s	TBM	31.35	5.81
	ELL	55.98	10.17
	WNS	77.47	13.70
	NAC	81.58	14.84
	MOX	90.20	15.86
	YAK	97.48	17.27
C.sse	VTG	54.69	9.46
	BRV	103.76	18.05
	RSW	124.66	21.61
	PRO	139.82	23.88

APPENDIX II

Even though the crustal model consists of five layers, only three main refractors exist: the basalts (1), the crystalline basement (2), and the deep crustal refractor (3). The following table lists the number of data points on a refractor (N), the number of crossing refraction lines (X), and the standard deviation between the observed and modeled first arrival times (σ_t).

TABLE AII.1 Standard Deviation of Arrival Times

Name	Refractor	N	X	σ_t (s)
USGS.sw	1	4	-	0.11
	2	7	-	0.14
	3	7	-	0.17
USGS.ne	1	5	-	0.11
	2	6	-	0.06
	3	7	-	0.10
S1.w	1	1	-	-
	2	4	2	0.10
S1.wsw	1	2	-	0.13
	2	4	3	0.21
S2.s	1	4	1	0.10
	2	1	1	-
	3	1	-	-
S2.sse	1	4	1	0.11
	2	2	1	0.14
S2.se	1	2	1	0.19
	2	4	1	0.14
S3.nw	1	1	-	-
	2	4	2	0.19
S3.e	1	2	2	0.11
	2	2	1	0.20
S3.se	1	3	-	0.18
	2	1	1	-

S4.n	1	2	-	0.30
	2	8	2	0.10
	3	2	-	0.01
S4.w	1	2	-	0.36
	2	4	-	0.05
S4.e	1	1	-	-
	2	2	1	0.01
	3	4	-	0.12
C.s	2	6	1	0.17
C.sse	2	3	3	0.28
	3	1	-	-